

POLITECNICO DI TORINO

Corso di Laurea Magistrale in
Ingegneria Energetica e Nucleare

Tesi di Laurea Magistrale

Advanced thermal comfort model based
on human body exergy balance



Relatori:

Prof. Marco Simonetti

Prof. Umberto Lucia

Candidata:

Stefania Li Crasti

A.A. 2017/2018

Abstract

This thesis project is focused on the description of an advanced thermal comfort model based on human body exergy balance.

Thermal comfort models have been widely studied since the beginning of the twentieth century, to provide an analytical formulation able to predict the human body response when it is exposed to a specific thermal environment.

The definition of the main existing thermal models represents the first part of the analysis. Afterwards, the choice of the model and the characterization of the body response have been done studying the un-steady state trend of two main variables: core temperature and skin-layer temperature.

The results obtained have been used to apply an exergy balance on human body and to carry out a new expression for its exergy efficiency.

Finally, the exergy analysis of human body has been linked with thermal comfort, through the Predicted Mean Vote index.

The analysis highlights the importance of setting up an exergy balance of human body to look for the parameters that influence thermal comfort within a specific ambient and to find if the body is sensitive to the energy quality and form.

Exergy concept could give us essential information on the importance of each type energy transfer effectively, hence without taking into account of the energy intrinsically present in all energy processes.

List of figures

Figure 1. PPD as a function of PMV	4
Figure 2. Schematic representation of the human body, with the intake of food, water and inspired air; and output of food, urine, expired air, vaporization through skin and heat release due to radiation and convection [8].....	6
Figure 3. Schematic view of the ThermoSEM model [10].....	7
Figure 4. Exergy consumption dependent on mean radiant temperature ($T_a = 20\text{ }^\circ\text{C}$) [2]	10
Figure 5. Exergy consumption as a function of air and mean radiant temperature [2].	10
Figure 6. Modelling of human body consisting of two subsystems: core and shell [11]	12
Figure 7. Heat and mass flow in two-node human body model: 1 – conduction between core and skin compartment, 2 – blood flow between core and skin compartment, 3 – thermal radiation, 4 – water perfusion and sweating, 5 – convective heat and mass transfer, 6 – breathing [12].....	13
Figure 8. Energy interaction between the human body and the surrounding environment [7]	14
Figure 9. Core and skin temperature trend in time	26
Figure 10. Core temperature trend.....	27
Figure 11. Skin temperature trend.....	27
Figure 12. Heat transfer rate between core and skin in time.....	28
Figure 13. Core e skin temperature trend in time (case 2)	29
Figure 14. Heat transfer rate between core and skin in time.....	30
Figure 15. Core e skin temperature trend in time (case 3)	30
Figure 16. Core temperature trend.....	31
Figure 17. Heat transfer rate between core and skin in time.....	31
Figure 18. Skin-layer temperature trend with different mean radiant temperatures ...	33
Figure 19. Heat transfer between core and skin with different mean radiant temperatures	33
Figure 20. Core temperature trend with higher temperatures	34

Figure 21. Exergy interaction between the human body and the surrounding environment [7]	35
Figure 22. Human body exergy efficiency in time	44
Figure 23. Convection, radiation and evaporation exergy rate on time	44
Figure 24. Exergy efficiency in time with different mean radiant temperatures	45
Figure 25. Exergy efficiency in time with different air temperatures	46
Figure 26. Exergy efficiency with different radiation heat transfer coefficients	47
Figure 27. Final values of exergy efficiency as function of radiative heat transfer coefficient.....	47
Figure 28. Exergy efficiency with different convective heat transfer coefficients.....	48
Figure 29. Final values of exergy efficiency as function of convective heat transfer coefficient.....	48
Figure 30. Exergy efficiency as a function of both mean radiant and air temperatures	49
Figure 31. 3D plot of exergy efficiency as a function of both mean radiant and air temperatures	50
Figure 32. Exergy efficiency variation with $v_{air} = 0.08$ m/s.....	51
Figure 33. Exergy efficiency variation with $v_{air} = 0.3$ m/s.....	51
Figure 34. PMV trend in time.....	53
Figure 35. PMV trend with different mean radiant temperatures	54
Figure 36. Final PMV values with different mean radiant temperatures.....	54
Figure 37. PMV as a function of both mean radiant and air temperatures.....	55
Figure 38. PMV and exergy efficiency	56
Figure 39. Exergy efficiency as a function of PMV.....	57
Figure 40. Exergy efficiency as a function of PMV for different air temperatures.....	57
Figure 41. Radiation exergy transfer rate for different radiation area factors.....	60
Figure 42. Exergy efficiency with $f_{eff} = 0.5$	61
Figure 43. Exergy efficiency with $f_{eff} = 0.9$	61
Figure 44. PMV and exergy efficiency with $f_{eff} = 0.5$	62
Figure 45. PMV and exergy efficiency with $f_{eff} = 0.9$	63

Contents

Introduction.....	1
1. A review into thermal comfort	3
1.1. Preface	3
1.2. The heat-balance approach	3
1.3. Criticism on heat-balance based models.....	4
1.4. Adaptive approach.....	5
1.5. Advanced thermo-physiological models	5
1.6. Exergy and human body	8
1.7. Exergy and thermal comfort	8
2. The two-node thermal model.....	12
2.1. Choice of the model.....	12
2.2. Energy balance.....	13
2.3. Solution of the two-node model	15
3. Solution of the two-node thermal model.....	22
3.1. Finite differential equations.....	22
3.2. Case study	24
3.3. Core and skin-layer temperatures: results and discussion.....	26
3.4. Generalizations	32
4. Human body exergy efficiency	35
4.1. Exergy balance.....	35
4.2. Exergy efficiency: definitions.....	36
4.3. Reference temperature	42

4.4.	Exergy efficiency: results and discussion.....	43
4.5.	Exergy efficiency variation with different mean radiant and air temperature	45
4.6.	Exergy efficiency trend according to radiative and convective heat transfer coefficients.....	46
4.7.	Exergy efficiency and environment temperatures.....	49
4.8.	Exergy efficiency and mean air velocity	50
5.	<i>Exergy efficiency and thermal comfort.....</i>	52
5.1.	PMV trend.....	52
5.2.	Exergy and PMV.....	55
5.3.	Sensitivity analysis on f_{eff}	58
6.	<i>Conclusions</i>	64

Introduction

Thermal comfort has been defined as the condition of mind which expresses satisfaction with the thermal characteristics of the surrounding environment and is assessed by subjective evaluation (ASHRAE, standard 55). Maintaining comfort conditions for occupants in buildings or enclosures is one of the main goals of HVAC engineering, which aim is controlling heating, ventilation and cooling parameters providing thermal neutrality sensation for human body.

One of the most important contributors to the development and usage of an energy balance model for human body was P.O. Fanger, who created a predictive model from laboratory and climate chamber research. The Predictive Mean Vote Model (PMV) is used till nowadays to assess thermal comfort and it is based on a seven points scale (from -3 to +3), describing a specific thermal sensation, from the coolest (-3) to the hottest (+3).

Fanger's aim was to present a method used to predict, for any kind of activity level and clothing insulation, all those combinations of environment thermal factors for which the largest possible amount of people experiences thermal comfort [1].

Other comfort models were developed taking into account people's adaptation and expectation within a specific environment. The so-called Adaptive Model differentiates between natural and mechanical ventilated buildings to analyse how the outdoor climate influences the indoor conditions, hence occupants' preferences and tolerance. Since over the last twenty years, also the exergy analysis of built environment has become well recognized by engineers and scientists involved in heating and cooling load calculations and indoor climate. The concept of exergy is introduced in the second law of thermodynamics: every energy transfer and conversion is accompanied by exergy and, while energy is conservative in its processes, exergy is non-conservative, due to the irreversibility which cause entropy production, hence exergy consumption. Exergy is a measure of energy quality and it is defined as the maximum amount of useful work that can be extracted from a system only interacting with its own environment, or the minimum work required to obtain a given state from environmental conditions.

Indeed, the human body is considered as a thermodynamic open system, exchanging heat with the surrounding environment (mainly by convection and radiation) and losing heat by evaporation of body fluids. Since the energy exchange defines thermal sensation, the path of energy, mass and the associated transformations should be considered. The human thermal model could be further studied from an exergetic point of view; in this case energy quality is a pseudo-thermodynamic state of system and is a function of the environment [2]. The study of our organism from this viewpoint could give us a better understanding of the relation between human thermal comfort and the built environment, leading to increasingly sustainable solutions for heating, cooling and ventilating systems.

The goal of this research is to analyse the human body response within a specific thermal environment through exergy analysis. A new definition of exergy efficiency has been given and the existence of a relationship between exergy efficiency and thermal comfort has been investigated, to understand if it could be an useful instrument to predict human body thermal sensation.

1. A review into thermal comfort

1.1. Preface

Thermal comfort has been defined as “a state in which there are no driving impulses to correct the environment by behaviour”[3] or “the condition of mind in which satisfaction is expressed within the thermal environment”[4].

Thermal sensation is influenced by many factors that affect the comfort perception among people; it depends also on the behavioural and physiological adaptation of people and that is why thermal satisfaction cannot be regulate by an absolute standard. In general, comfort occurs when body temperatures are held within close ranges, the skin moisture is very low and the physiological regulation is minimized. [5]

Thermal comfort has been discussed till 1930s because of the need to reduce energy consumption and, during decades had been developed mainly two main approaches: the heat-balance model and the adaptive one, which are now the basis of international standards (ISO 7730, ASHRAE 55, etc.)

In this first chapter both models will be discussed, together with a third way to approach thermal comfort within the indoor environment, which applies the exergy concept to the human body system.

1.2. The heat-balance approach

Important theories on human body heat exchanges were developed by Fanger [6] around 1970. He proposed an energy balance equation for human body, stating that human body moves always towards thermal equilibrium, whatever conditions it is exposed to.

Contemporary, he defined six parameters influencing thermal comfort; four of them are related to the environment (air temperature, mean radiant temperature, relative humidity and air speed), two are personal factors (metabolism and clothing resistance). Through numerous laboratory experiences in a climate chamber, Fanger presented a method to predict, for any type of activity level and clothing, all those combinations of

thermal factor for which the largest percentage of people feel satisfied.

The *Predicted Mean Vote* (PMV) index is based on Fanger's comfort equation and it defines the mean thermal sensation on a 7 points scale (from -3 to +3), each of them describing a specific thermal sensation, from the coolest (-3) to the hottest (+3), for given combination of environmental parameters.

Predicted Percentage of Dissatisfied (PPD) can be calculated as:

$$PPD = 100 - 95e^{(-0.03353 PMV^4 - 0.2179 PMV^2)} \quad (1.1)$$

and its dependency from PMV is shown in the figure 1 below.

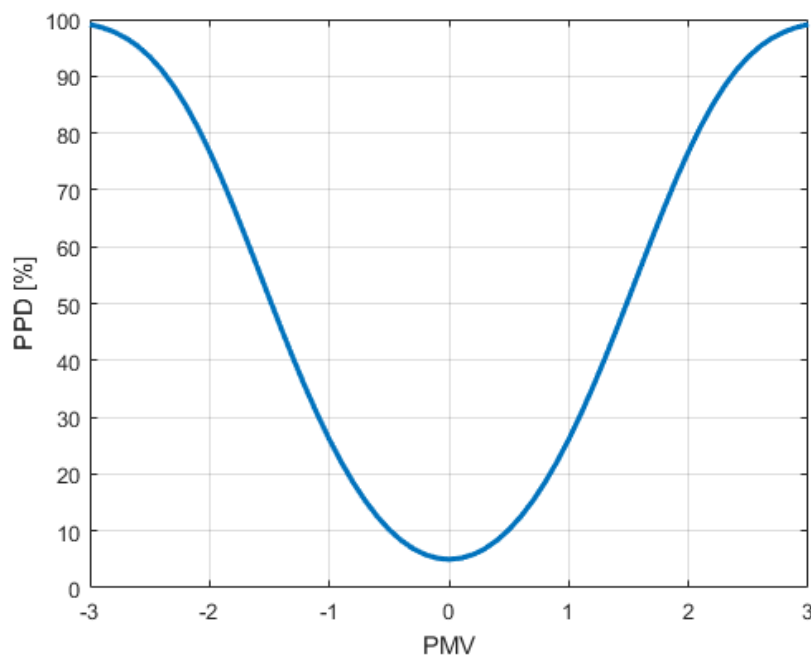


Figure 1. PPD as a function of PMV

Thermal comfort was then defined as the condition in which there is a percentage of dissatisfied lower than 10 %, hence PMV between -0.5 and 0.5.

The PMV-PPD model presented by Fanger was largely accepted and it widely used till nowadays for design and assessment of thermal comfort.

1.3. Criticism on heat-balance based models

The following studies showed that models based on steady state approach are sensitive and accurate only for human involved in near-sedentary activity. Moreover, the models

seem to oversimplify the role of metabolic rate and clothing insulation. The assumption of steady-state laboratory conditions does not take into account of the impact of physiological and cultural factors as well as people adaptation and expectations within a specific ambient. Furthermore, various field study showed that in some conditions, a large number of people feel no thermal discomfort, even if the thermal sensation is outside the three central categories of the 7-points scale.

1.4. Adaptive approach

Adaptive model derives from field studies, having the aim to examine the real range of acceptability of thermal environment, which depends strongly on occupants' behaviour psychological expectations and adaptation. Therefore, the approach is based on the assumption that adaptive factors play a central role in occupants' perception and definition of thermal comfort.

Moreover, perception discrepancies were found among occupants of naturally and mechanically ventilated buildings. In particular, for naturally ventilated buildings, the PMV model was unable to predict the indoor comfort parameters, because it could not justify the strong dependency of indoor temperature from the temperature outside the building envelope. This relation could be only examined through field based studies, considering the adaptation skill of the occupants of naturally ventilated buildings, which are usually subjected to a wider range of temperatures than the occupants of mechanical ventilated buildings. Furthermore, their thermal expectations within that building are lower, such that they are experienced in performing behavioural changes to restore their comfort.

Nowadays, adaptive thermal comfort is an optional method to the PMV model for the application to natural ventilated buildings.

1.5. Advanced thermo-physiological models

Parallely to Fanger's one, other advanced thermal modes were presented. These approaches are based on PMV-PPD model but they had been used to take into account

the dynamic character of thermal conditions, hence to conduct a transient analysis for human body system.

In these models, the human body is modeled as composed of several layers.

Through the two-node model, developed by Gagge and used together with heat balance equations developed by Gagge and Nishi [7], the thermal behaviour of human body was simulated as two cylindrical subsystems: the core and the shell (skin-layer). While the core temperature has an almost constant temperature nearly 37 °C, the skin temperature is subjected to variations due to the surrounding environmental temperature and humidity. The model will be largely explained in section 2.1.

Gradually, the non-uniformity and dynamicity of the real thermal world led to an increasing complexity of the models. The whole shape of human body is extremely complex and the temperature of various parts of the body are different; in particular the body core temperature is almost constant, but the temperature of peripheral parts such as hands and foot varies and its variation is highly dependent on the surrounding thermal conditions; the blood circulation and the conduction between core and skin became central factors in the analysis.

Various scientists developed different thermal model to try to take into consideration the complexity of human body and its non-uniform temperature distribution.

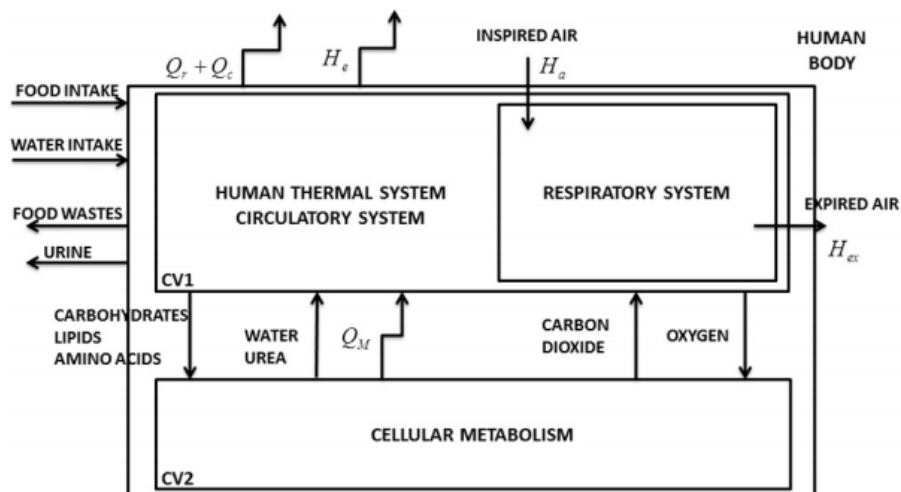


Figure 2. Schematic representation of the human body, with the intake of food, water and inspired air; and output of food, urine, expired air, vaporization through skin and heat release due to radiation and convection [8]

For example, Mady, Ferreira and Yanagihara [9] suggested a division of the body in 15 cylinders, representing the head, neck, trunk, arms, forearms, hands, thighs, legs and feet. Each cylinder has a characteristic combination of some types of tissues (skin, fat, muscle, bone, brain, viscera, lung and heart), ordered respecting the real succession from exterior layer to the internal one. Moreover, each cylinder is thermally isolated in the upper and lower basis and some of these segments communicate only by means of blood circulation.

Mady and Oliveira [8] indicated a simplified representation of human body in which the body is modelled as two control volumes interacting with each other and with the surrounding environment. The first control volume, named CV1, represents the thermal and respiratory system and the second CV2 the cellular metabolism (figure 2).

With recent progresses in this field, the application of computational fluid dynamics has been used to developed new advanced models, of which one example is shown in figure 3.

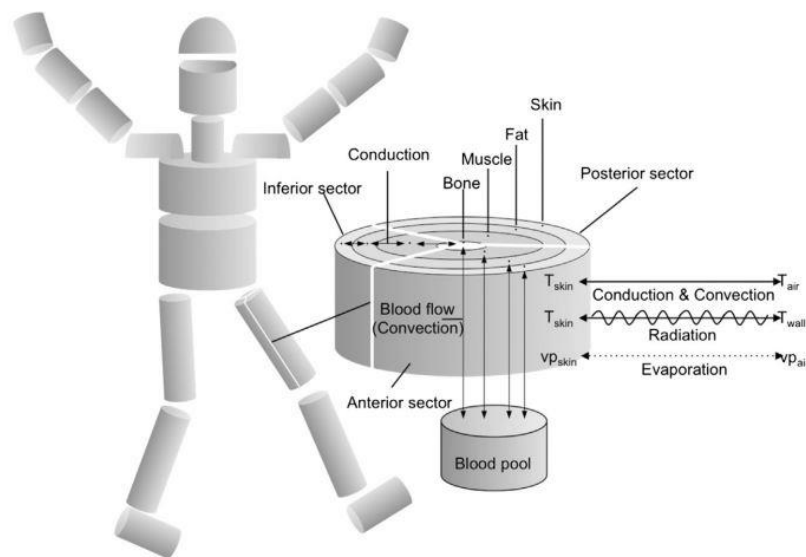


Figure 3. Schematic view of the ThermoSEM model [10]

The model, called ThermoSEM, splits the human body in 18 cylinders and one hemisphere, and each of them is subdivided in many layers, that have their own characteristic composition in terms of different tissues the layer is made-up by.

1.6. Exergy and human body

Animals, including human beings, use organic matters to live. Food contains a lot of exergy in chemical form, destroyed and transformed by our organism. This transformations bring out a lot of exergy that is used later to permit the motion of muscles but also to keep the body temperature almost constant at a value which allows bio-chemical reactions take place and avoids serious health disorders or even death risk. This temperature, as we know by our own unconscious experience, is generally higher than environmental temperature.

The fact that humans, as other mammals, tend to maintain a constant body temperature implies that energy exchanges occur between surrounding environment and body.

Many HVAC engineers have wondered whether the human body, being a thermal system, is sensitive to energy quality or not, in other words if a correlation between human body physiology and exergy exists.

The first law of thermodynamics, which for definition is a quantitative balance of energy processes, is not able to take into account the quality of body thermal mechanisms; in the light of this, the second law of thermodynamics could be an important instrument to analyse energy quality dissimilarity among thermo-regulatory systems.

The second law can be expressed as inequality between entropy variations. Applying it to the isolated system composed by the human body and its surrounding environment, it can be written as:

$$\Delta S_{sist} = \Delta S_{body} + \Delta S_{env} \geq 0 \quad (1.2)$$

The equality is verified only in case of reversible processes, characterized by entropy conservation; real processes are all irreversible, such that a certain amount of entropy is always generated, resulting in ΔS_{sist} greater than 0.

1.7. Exergy and thermal comfort

Knowing that the exergy of a system increases when its temperature, pressure and/or chemical potential differs from the ones of the environment considered as 'dead state', it is possible to suppose that the creation of irreversibility plays a central role in the

determination of thermal comfort sensation.

Therefore, human body considered as an open thermodynamic system could experience thermal discomfort if the interaction with the surrounding ambient causes an increment of its generated entropy, hence of its exergy loss.

In the latest twenty years, this reasoning has moved many scientists to look for a relationship between destroyed exergy and thermal comfort and, using the thermo-physiological models discussed in section 1.5., different analysis of human body based on 2nd law of thermodynamics had been carried out.

A complete transient analysis has been done by Shukuya [11]. He set up the water balance, the energy and entropy balance for human body system and finally he combined them to obtain a full exergy balance. It is interesting to notice that he identified the two reasons of exergy consumption: the thermal dispersion caused by the temperature difference between body core, shell and clothing surface and the dispersion of liquid water into water vapour of the surrounding environment. Indeed, he included in his balance a warm chemical contribution, produced by metabolism to allow cellular activity. The exergy consumption was then calculated as difference between the input quantities and the output ones.

Prek [12] used a different way to obtain the exergy consumption of human body: the exergy destruction was calculated for each heat and mass transfer process separately, with respect to a consistent reference state, common to every process.

Wu and Olesen [13] developed a novel formula to calculate human body exergy consumption, taking into account the aspect of external irreversibility, that was previously treated with confusion by other authors.

However, all the researches turned out very similar results, associating thermal comfort to exergy consumption rate and affirming that thermal comfort condition occurs contemporary to a minimum human body exergy consumption rate.

In Figure 4 and 5 are shown the results obtained by Prek. By increasing room temperature, the exergy consumption rate decreases till a minimum at certain temperatures and it is reached at a specific combination of mean radiant temperature and air temperature.

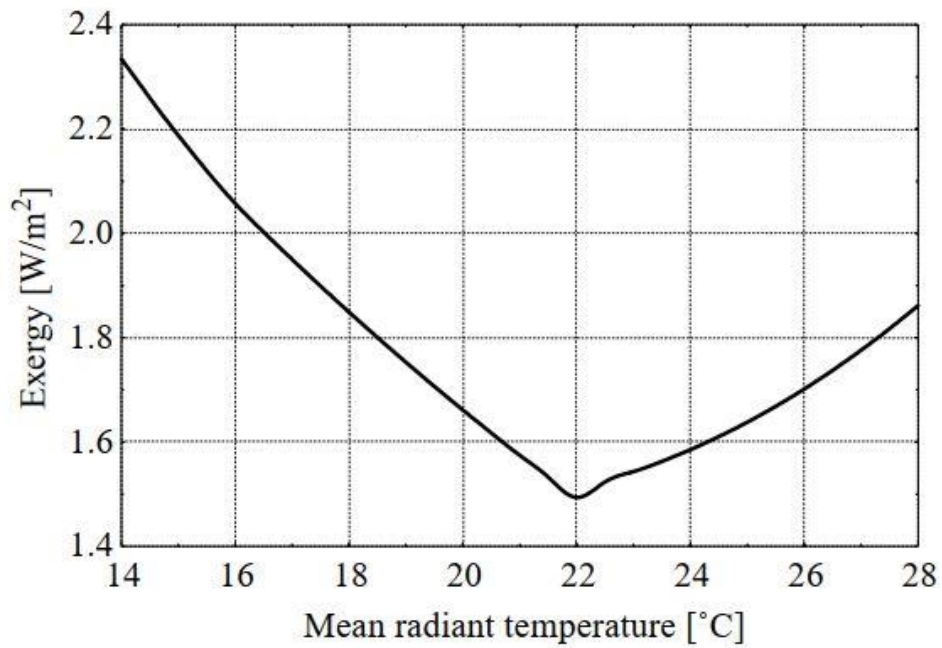


Figure 4. Exergy consumption dependent on mean radiant temperature ($T_a = 20^{\circ}\text{C}$) [2]

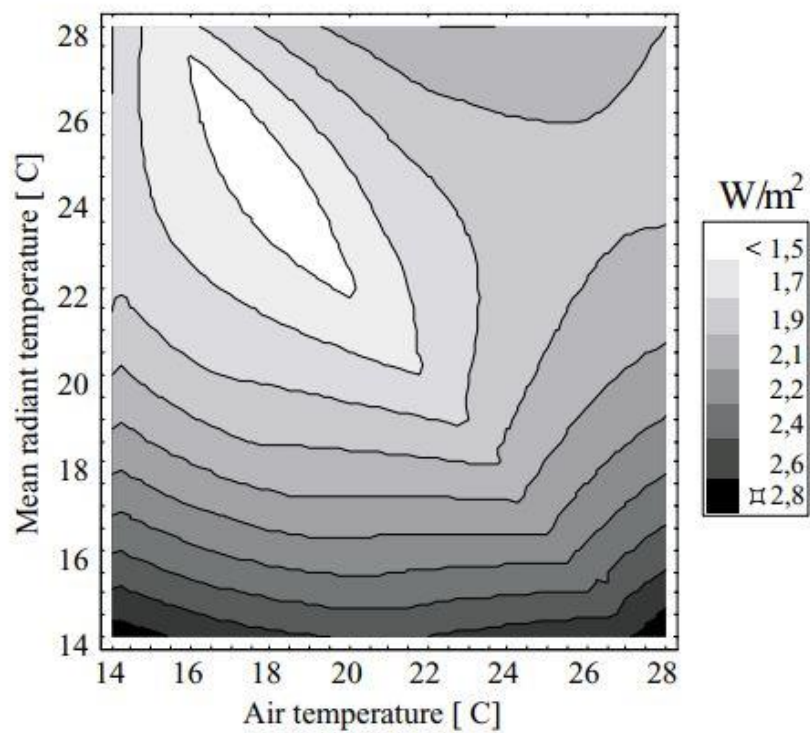


Figure 5. Exergy consumption as a function of air and mean radiant temperature [2]

At lower temperatures, shivering causes higher exergy destruction and it is a result of the increased difference between body core and skin-layer temperature. Similarly, when the environment becomes hotter, the exergy consumption rate increase is caused by sweating and due to the difference between actual and set-point skin and/or core temperature.

Moreover, the increment of exergy destruction rate is faster when room temperature moves towards higher values. Hence, the production of sweat has a stronger influence on exergy analysis than shivering.

2. The two-node thermal model

2.1. Choice of the model

Theoretically speaking it should be possible to set up a human thermal model taking into consideration the complexity of human body and surely obtaining improvements of the accuracy, but it will lead to more complicate equations and hence, more unknown variables that have to be assumed.

For this reason the two-node thermal model has been used in this research, as many researchers and engineers have done in the field of heating and cooling in buildings [2], [7], [11]-[15].

The thermal behaviour of human body has been simulated as two subsystems: the core and the shell (skin layer). The core temperature has been considered almost constant nearly 37 °C, while the skin temperature is subjected to variations due to environmental temperature and humidity and to the metabolism level. The two subsystems exchange energy passively through direct contact and through peripheral blood flow. Core and skin temperature and skin wetness have been supposed to be uniform above all the considered layers (figure 6).

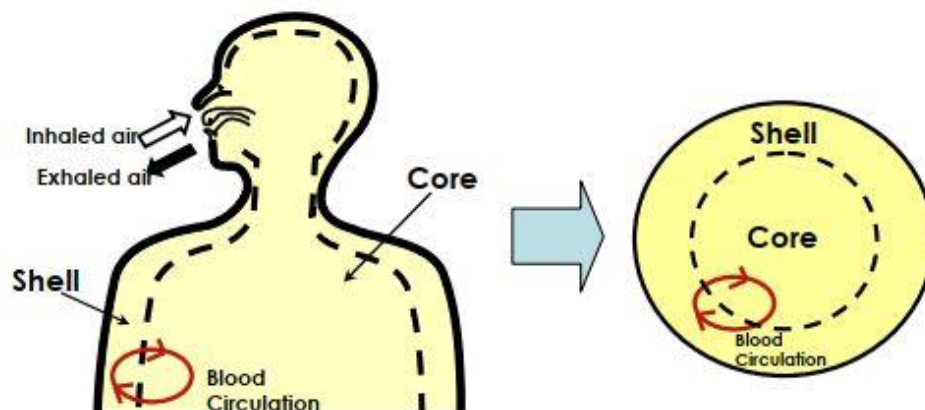


Figure 6. Modelling of human body consisting of two subsystems: core and shell [11]

Metabolic heat production at the core subsystem is released to the environment in two ways. The major one is the transfer of heat to the skin by blood flow and heat

conduction, followed by release from the skin to the environment by convection, radiation, and evaporation. The minor pathway is the direct release of heat (and mass) to the environment through respiration (figure 7).

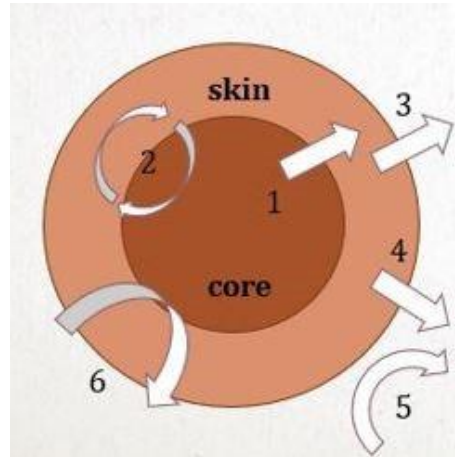


Figure 7. Heat and mass flow in two-node human body model: 1 – conduction between core and skin compartment, 2 – blood flow between core and skin compartment, 3 – thermal radiation, 4 – water perfusion and sweating, 5 – convective heat and mass transfer, 6 – breathing [12]

Our organism regulates blood distribution by vasoconstriction and vasodilatation in order to increase or decrease heat loss to the environment: during work, blood carries the produced extra-heat to the surface where higher skin temperature increases heat loss through convection and radiation; on the contrary, during cold stress vasoconstriction takes place. Moreover, in hot environments, convective and radiative heat transfers from the body decrease due to the small difference between skin temperature and ambient temperature, so the heat release is controlled by water diffusion and evaporation (latent heat) [16].

2.2. Energy balance

Let's assume that a human body system is situated in a room with known air temperature, air relative humidity, mean radiant temperature and air velocity, the outside air temperature; the human body is clothed, with a known clothing thermal

resistance. We can set up the transient energy balance for this system and its schematic view is shown in figure 8.

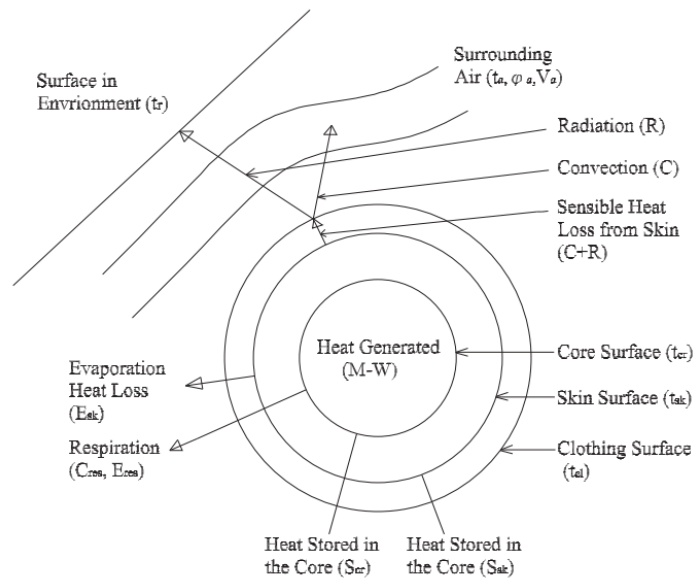


Figure 8. Energy interaction between the human body and the surrounding environment [7]

The heat generated within the body system must be equal to the net energy transfer into the surrounding environment, with a surplus or deficit represented by the storage in the body.

The energy balance equation is given by:

$$M - W = Q_{res} + Q_{sk} + S = (C_{res} + E_{res}) + (E_{sk} + C + R) + S \quad (2.1)$$

where:

M represents the rate of metabolic energy generation;

W is the external work;

C_{res} is the sensible heat rate lost by respiration;

E_{res} is the latent heat rate lost by respiration;

E_{sk} is the evaporative heat loss rate;

C is the convective heat transfer rate;

R is the radiative heat transfer rate;

S is the heat storage rate in the body.

There is also conduction in reality (from feet to the floor), but it is neglected and implicitly considered in a portion of convection. All the quantities are expressed in Watt.

2.3. Solution of the two-node model

The two-node energy balance equations are expressed taking into account separately the two subsystems. The solution to the equations has been done following the procedure explained by Shukuya [17], that will be recalled in this section.

At the core subsystem:

[Thermal energy generated by metabolism] =
= [Thermal energy stored in the body core] +
+ [The difference in enthalpy between exhaled and inhaled humid air] +
+ [The difference in enthalpy between blood flowing out from the body core and that flowing into the skin layer]

At the skin subsystem:

[The difference in enthalpy between blood flowing out from the body core and that flowing into the skin layer] =
= [Thermal energy stored in the skin layer] +
+ [Heat transfer from the skin to the clothing layer] +
+ [Thermal energy dispersed by evaporation of sweat]

The first equation can be explicated as:

$$(q_{met} + q_{shiv}) = Q_{cr} \frac{dT_{cr}}{dt} + (c_{res} + e_{res}) + K(T_{cr} - T_{sk}) \quad (2.2)$$

and the second:

$$K(T_{cr} - T_{sk}) = Q_{sk} \frac{dT_{sk}}{dt} + \frac{1}{R_{cl}} (T_{sk} - T_{cl}) + w(F_{pcl} f_{cl} I_r h_c) [p_{sks}(T_{sk}) - p_a(T_a)] \quad (2.3)$$

The second term of the right side of equation 2.3 could be expressed also as:

$$\frac{1}{R_{cl}}(T_{sk} - T_{cl}) = f_{cl}h_r(T_{cl} - T_{mr}) + f_{cl}h_c(T_{cl} - T_a) \quad (2.4)$$

Moreover, the equations are referred to one-square meter surface area of human body, in an infinitesimally short period of time dt , in the unit of second.

2.3.1. Metabolic energy emission rate

The metabolic energy emission rate is expressed as:

$$q_{met} = 58.2 M(1 - \eta) \quad (2.5)$$

where M is the rate of metabolic energy emission and its values varies according the activity level. For sedentary posture $M = 1.0$ and the average human body emits heat at a rate of 58.2 W/m^2 .

η is the ratio of external work to the total metabolic thermal emission rate and its value is calculated starting from the value of M : for $M < 1.4$, $\eta = 0$; for $1.4 \leq M < 3$, $\eta = 0.1$ and $\eta = 0.2$ for $M \geq 3$.

2.3.2. Shivering energy generation rate

The shivering thermogenesis occurs under cold environment conditions. q_{shiv} is the rate of energy generation by shivering and derives from:

$$q_{shiv} = 19.4(T_{sk_{set}} - T_{sk})(T_{cr_{set}} - T_{cr}) \quad (2.6)$$

with $T_{sk_{set}} = 34.1 \text{ }^\circ\text{C}$ and $T_{cr_{set}} = 36.8 \text{ }^\circ\text{C}$. These values have been assumed in the calculation as set-point temperatures kept in the normal physiological condition to allow thermal homeostasis. T_{sk} and T_{cr} are the skin layer temperature and core temperature respectively.

The two temperature differences in equation 2.6 regulate the shivering process: if $(T_{sk_{set}} - T_{sk}) \leq 0$ or $(T_{cr_{set}} - T_{cr}) \leq 0$ then $q_{shiv} = 0$. So, only when $T_{sk} \leq T_{sk_{set}}$ and $T_{cr} \leq T_{cr_{set}}$, $q_{shiv} \neq 0$ and shivering thermogenesis occurs.

2.3.3. Body core and skin-layer heat capacity

The heat capacity of body-core and skin layer Q_{cr} and Q_{sk} are in the unit of $J/(m^2K)$. They are determined by a nondimensional factor, ratio of skin-layer mass to the total body mass, α_{sk} , through a formula developed by Wang [18]:

$$\alpha_{sk} = 0.0418 + \frac{0.745}{\dot{v}_{bl} + 0.585} \quad (2.7)$$

where \dot{v}_{bl} is the blood flow rate between body core and skin layer in $[L/m^2h]$ and it can be evaluated as:

$$\dot{v}_{bl} = \frac{6.3 + c_{dil}(T_{cr} - T_{cr,set})}{1 + \sigma_{tr}(T_{sk,set} - T_{sk})} \quad (2.8)$$

The factors c_{dil} and σ_{tr} are $75 \leq c_{dil} \leq 225$ and $0.25 \leq \sigma_{tr} \leq 0.75$. According to Gagge [7], the values of these two factors have not much influence on the final body-core and skin layer temperature under a constant environment, but do influence the way in which those final temperatures are reached. Shukuya [19] choose for his calculation values of 100 and 0.25 respectively, while Prek [12] used 200 and 0.5. However, the difference in the final temperatures between the two cases is lower than 1%. In this analysis the values assumed by Prek have been used.

Regarding the temperature differences found in \dot{m}_{bl} equation, they are considered as “signals” that the human body sends when the core or skin temperature is higher (or lower) than the set temperature. In particular:

- Warm signal for core: $T_{cr} - T_{cr,set}$
- Warm signal for skin: $T_{sk} - T_{sk,set}$
- Cold signal for core: $T_{cr,set} - T_{cr}$
- Cold signal for skin: $T_{sk,set} - T_{sk}$

The warm/cold signals rule thermoregulation mechanisms, hence the increase and reduction of blood flow from core compartment to skin-layer.

Equation 2.7 indicates that the ratio α_{sk} becomes larger as the blood flow rate decreases and this results in a decrement of skin layer temperature. As it has been explained previously, one of thermoregulation responsible is blood, and the variation of its flow rate direct to the skin is the mechanism that permit to control the body-core temperature.

Q_{cr} and Q_{sk} are calculated as:

$$Q_{cr} = (1 - \alpha_{sk}) \frac{M_{body}}{A_{Du}} c_{p,body} \quad (2.9)$$

$$Q_{sk} = \alpha_{sk} \frac{M_{body}}{A_{Du}} c_{p,body} \quad (2.10)$$

where M_{body} is the body mass [kg], A_{Du} is human body surface area [m^2] and $c_{p,body}$ is specific heat capacity of human body, taken from literature and equal to 3470 J/(kgK).

The body surface area has been calculated from Dubois' formula (equation 2.11), though a lot of relations to evaluate it exist and almost all of them express the body surface area as a function of height H [cm] and body mass M_{body} [kg].

$$A_{body} = 0.007184 H^{0.725} M_{body}^{0.425} \quad (2.11)$$

2.3.4. Sensible and latent enthalpy of respiration

The sum of c_{res} and e_{res} in the first equation, multiplied by the infinitesimal period of time dt is the difference in enthalpy between exhaled and inhaled humid air including the latent term. Their expression is given as:

$$c_{res} = 0.0014(58.2M)(T_{sk,set} - T_a) \quad (2.12)$$

$$e_{res} = 0.0173(58.2M)[5.87 - \varphi_a p_{sa}(T_a)] \quad (2.13)$$

where T_a is the air temperature, φ_a is the surrounding air relative humidity (dimensionless) and $p_{sa}(T_a)$ is the saturated vapour pressure at temperature T_a in the unit of kPa, given by:

$$p_{sa}(T_a) = \frac{e^{25.89 - \frac{5319}{T_a}}}{1000} \quad (2.14)$$

2.3.5. Heat transfer coefficient

K is the overall heat transfer coefficient between the body core and the skin layer, calculated from the empirical formula:

$$K = k + c_{p,bl} \rho_{bl} v_{bl} = k + 1.163 \dot{v}_{bl} \quad (2.15)$$

The values for $c_{p,bl}$ (blood specific heat capacity at constant pressure), ρ_{bl} (blood density) and K have been taken from literature: 4.186 J/(kgK), 1 g/mL and 5.28 W/(m^2K) respectively; v_{bl} is the blood flow rate in the unit of mL/(m^2s).

2.3.6. Clothing thermal resistance

Clothing thermal resistance R_{cl} [m^2K/W] is associated with the level of clothing insulation I_{cl} , expressed by the unit of *clo*, through the formula:

$$R_{cl} = 0.155I_{cl} \quad (2.16)$$

meaning that 1 *clo* = 0.155 $W/(m^2K)$.

2.3.7. Skin wetness factor

It is the ratio of fully wet skin surface area to the whole skin surface area.

$$w = 0.06 + 0.94 \frac{E_{rsw}}{E_{max}} \quad (2.17)$$

This equation implies that, if E_{rsw} is null (there is no sweat secretion), 6% of the body surface area is fully wet and 94% is fully dry; if sweat is produced the skin wetness factor increases above 6% and its increment is proportional to the sweat secretion rate E_{rsw} , expressed through equation 2.18:

$$E_{rsw} = 170(T_b - T_{b,set})e^{\frac{T_{sk} - T_{sk,set}}{10.7}} \quad (2.18)$$

T_b and $T_{b,set}$ represent the overall body temperature in the actual condition and the overall body temperature in the initial condition and their values are obviously dependent on T_{cr} , $T_{cr,set}$, T_{sk} and $T_{sk,set}$ values:

$$T_b = \alpha_{sk}T_{sk} + (1 - \alpha_{sk})T_{cr} \quad (2.19)$$

$$T_{b,set} = \alpha_{sk}T_{sk,set} + (1 - \alpha_{sk})T_{cr,set} \quad (2.20)$$

This time, to apply correctly eq. 2.18 all temperatures must be expressed in [$^{\circ}C$].

Moreover, another assumption has to be done: if $T_b \leq T_{b,set}$ then $E_{rsw} = 0$; this means that sweat secretion occurs only if $T_b > T_{b,set}$, in which case $T_{sk} > T_{sk,set}$.

E_{max} is the maximum rate of evaporation from the skin surface, including the effect of clothing, expressed through equation 2.21.

$$E_{max} = F_{pcl}f_{cl}I_r h_c [p_{sks}(T_{sk}) - p_a(T_a)] \quad (2.21)$$

where F_{pcl} is the dimensionless permeation efficiency factor of clothing, calculated as:

$$F_{pcl} = \frac{1}{R_{e,cl}f_{cl}I_r h_c + 1} \quad (2.22)$$

$R_{e,cl}$ is the clothing moisture resistance in $[m^2kPa/W]$ and it is related to the clothing insulation through the factor i_c , ratio of thermal resistance to the moisture resistance with respect to clothing; in other words, when i_c is lower, the clothing is less permeable:

$$R_{e,cl} = \frac{R_{cl}}{I_r i_c} \quad (2.23)$$

f_{cl} is the ratio of total surface area to naked body surface area, which is given as:

$$f_{cl} = 1 + 0.15I_{cl} \quad (2.24) \quad \text{or} \quad f_{cl} = 1 + 0.3I_{cl} \quad (2.25)$$

I_r is the ratio of moisture transfer coefficient to convective heat transfer coefficient, derived from Lewis relationship and taken to be $16.5 \text{ } ^\circ\text{C}/kPa$, constant under a constant atmospheric pressure of 101.3 kPa .

The convective heat transfer coefficient has been taken as the maximum between two different values and its unit is $[W/(m^2K)]$:

$$h_c = 5.66 \left(\frac{q_{met}}{58.2} - 0.85 \right)^{0.39} \quad (2.26)$$

$$h_c = 8.6v_{air}^{0.53} \quad (2.27)$$

being v_{air} the air velocity in the surrounding environment.

Considering equations 2.23, 2.24, 2.26 and 2.27, and taking as reference the studies done by Nishi and Gagge [7], the expression for F_{pcl} becomes:

$$F_{pcl} = \frac{1}{1+0.143I_{cl}f_{cl}h_c} \quad (2.28)$$

implying that i_c is assumed equal to 1.084.

In the equation of E_{max} , $p_{sks}(T_{sk})$ also appears. It is the saturated vapour pressure at the skin temperature T_{sk} , calculated as previously described for the saturated vapour pressure at temperature T_a . $p_a(T_a)$ is the partial vapour pressure of the surrounding air expressed as $\varphi_a * p_{sa}(T_a)$.

2.3.8. Linearized radiative heat transfer coefficient

Linearized radiative heat transfer coefficient [12] can be determined as:

$$h_r = 4f_{eff}\varepsilon\sigma \left(\frac{T_{cl}+T_{mr}}{2} \right)^3 \quad (2.29)$$

with ε overall emittance of the clothed body surface and σ is Stephan-Boltzmann constant equal to $5.67 \times 10^{-8} \text{ W}/(\text{m}^2\text{K}^4)$.

In the energy balance equation for skin subsystem, we find the sum of radiative and convective energy transfer rate and from this equation we can find the expression for T_{cl} average clothing temperature in [K]:

$$q_{dry} = \frac{1}{R_{cl}}(T_{sk} - T_{cl}) = f_{cl}h_r(T_{cl} - T_{mr}) + f_{cl}h_c(T_{cl} - T_a) \quad (2.30)$$

After some mathematical operations, explicating the clothing temperature

$$T_{cl} = \frac{\frac{1}{R_{cl}}T_{sk} + f_{cl}h_rT_{mr} + f_{cl}h_cT_a}{\frac{1}{R_{cl}} + f_{cl}(h_r + h_c)} \quad (2.31)$$

we can substitute it into the general form of q_{dry} :

$$q_{dry} = F_{cl}f_{cl}(h_r + h_c)(T_{sk} - T_{op}) \quad (2.32)$$

where

$$F_{cl} = \frac{1}{1 + 0.155I_{cl}f_{cl}(h_r + h_c)} \quad (2.33)$$

and

$$T_{op} = \frac{h_rT_{mr} + h_cT_a}{h_r + h_c} \quad (2.34)$$

calling T_{op} operative temperature, which is the uniform temperature of an imaginary environment having air temperature equal to T_a and mean radiant temperature equal to T_{mr} .

3. Solution of the two-node thermal model

3.1. Finite differential equations

Our aim in this first part of the solution of the two-node model is to find core and skin-layer temperature trends in time, till they have reached the equilibrium with the thermal environment the human body system is exposed to.

The set of equations 2.2 and 2.3 is a differential non-linear system with two unknown variables T_{cr} and T_{sk} and its non-linearity comes from the fact that q_{shiv} , K , Q_{sk} , Q_{cr} and w are function of the unknown variables.

Because of this non-linearity the system is easy to be solved approximating the differential equations with the respective finite-differential equations.

The time t is a continuous variable, sum of a series of discrete time interval Δt :

$$t = [0, \Delta t, 2\Delta t, 3\Delta t, \dots, (n-1)\Delta t, n\Delta t, (n+1)\Delta t, \dots]$$

During the generic infinitesimal period of time dt , T_{cr} and T_{sk} are subjected to an infinitesimal variation dT_{cr}/dt and dT_{sk}/dt . These variations can be expressed using the finite difference approximation: being the two function T_{cr} and T_{sk} continuous and differentiable in the considered interval of time, we can seek an approximation of the first derivative of both the functions at a generic point t in $(0, t)$.

For an increment h sufficiently small and positive, we can assume that:

$$(\delta + T_i)(t) = \frac{T_i(t+h) - T_i(t)}{h} \quad (3.1)$$

is an approximation of dT_i/dt , where the subscript i refers to core or skin, indifferently. This approximation is called *backward finite difference*, because the calculation is done backward and the value of the function at the instant of time $n\Delta t$ depends also on itself ($T_i(t+h)$). If this form is chosen, then the equations are called *implicit*. They stand as a set of two simultaneous non-linear equations with two unknown variables. It should be easy to solve these equations, if the values of q_{shiv} , K , Q_{sk} , Q_{cr} and w are given. Because they are functions of the unknown variables, it is needed an iterative procedure until two values for T_{cr} and T_{sk} satisfy the equality of both sides of the equations.

Because of this reason, the *explicit* type of approximation has been used, called *forward finite difference* form. The derivative of the function is expressed as:

$$(\delta - T_i)(t) = \frac{T_i(t) - T_i(t-h)}{h} \quad (3.2)$$

In this case, the values of q_{shiv} , K , Q_{sk} , Q_{cr} and w are evaluated at the previous interval of time $(n-1)\Delta t$, using $T_{cr}(n-1)$ and $T_{sk}(n-1)$. Therefore, the numerical calculation is performed simply forward, step by step, without any iterative procedure required.

Both the forms are first order accurate, but the implicit form is more costly than the explicit one, since the function is non-linear and at any time we have to solve a non-linear problem to compute it [20]. While the implicit methods are characterized by better stability, explicit type of approximation are characterised by a strict constraint in the time interval: Δt has to be chosen short enough so that the result of calculation can always converge.

Considering a time interval which goes from $(n-1)\Delta t$ to $n\Delta t$ and substituting the finite differential expression in equation 2.2, T_{cr} has been found from:

$$\begin{aligned} T_{cr}(n) = & \left[1 - \frac{\Delta t K(n-1)}{Q_{cr}(n-1)} \right] T_{cr}(n-1) \\ & + \frac{\Delta t}{Q_{cr}(n-1)} [q_{met}(n-1) + q_{shiv}(n-1) - c_{res}(n-1) - e_{res}(n-1) \\ & + K(n-1)T_{sk}(n-1)] \end{aligned} \quad (3.3)$$

To consider the constraint in the definition of Δt , the factor in front of $T_{cr}(n-1)$ has to satisfy the condition:

$$\left[1 - \frac{\Delta t K(n-1)}{Q_{cr}(n-1)} \right] \geq 0 \quad (3.4)$$

which leads to:

$$\Delta t \leq \frac{Q_{cr}(n-1)}{K(n-1)} \quad (3.5)$$

Similarly, the finite differential equation for $T_{sk}(n)$ is:

$$\begin{aligned}
 T_{sk}(n) = & \left[1 - \frac{\Delta t K(n-1)}{Q_{sk}(n-1)} - \frac{\Delta t f_{cl} F_{cl} (h_r + h_c)}{Q_{sk}(n-1)} \right] T_{sk}(n-1) \\
 & - \frac{\Delta t w(n-1) f_{cl} I_r h_c F_{pcl}}{Q_{sk}(n-1)} p_{sks}(n-1) \\
 & + \frac{\Delta t}{Q_{sk}(n-1)} \left[K(n-1) T_{sk}(n-1) + f_{cl} (h_r + h_c) F_{cl} T_{op}(n-1) \right. \\
 & \left. + w(n-1) f_{cl} I_r h_c F_{pcl} p_a(n-1) \right]
 \end{aligned} \tag{3.6}$$

and, after some mathematical calculations, the constraint on Δt becomes:

$$\Delta t \leq \frac{Q_{sk}(n-1)}{K(n-1) + f_{cl} F_{cl} (h_r + h_c) + w(n-1) f_{cl} I_r h_c F_{pcl} \frac{p_{sks}(n-1)}{T_{sk}(n-1)}} \tag{3.7}$$

The whole procedure of calculation takes into account all the equations previously described.

3.2. Case study

The two-node model has been solved following the procedure originally indicated by Gagge et al. [7]. The first step done is the calculation of body-core, skin layer and clothing surface temperature. Afterwards, the calculated temperatures, accompanied by consistent boundary conditions, have been used to calculate a new efficiency index that will be discussed in the following chapter.

The model contains many physiologically dependent and independent terms and combines them to predict the physiology that occurs after a fixed exposure period to various environmental condition.

It has been assumed that a human body system, with initial body core temperature of 36.8°C and skin layer temperature of 34.1°C, is placed at the time $t = 0$ in a room of known thermal characteristics. The body has a well-known activity level and clothing thermal resistance.

The following assumptions have been done for the analysis:

-
- All the processes are external irreversible, which means that the exergy consumption is produced during the exergy transfer between the human body and the surrounding environment, and the exergy consumption produced within human body has been assumed to be zero;
 - The room ambient is much bigger than the body system, so that any heat and/or mass transfer between the two doesn't affect the thermal characteristics of the room, i.e. air temperature, mean radiant temperature and relative humidity of the room air are constant at the initial values;
 - Conduction between feet and floor is neglected and implicitly considered in a portion of convection;
 - External work is null.

The calculation has been implemented with MATLAB software, running the script and evaluating the transient of T_{cr} and T_{sk} , till the equilibrium is reached.

In table 1 are summarized the initial assumptions that have been done.

	<i>Value</i>
Skin set temperature	34.1 °C
Core set temperature	36.8 °C
Metabolism	1.1 <i>Met</i>
Clothing insulation	0.63 <i>clo</i>
Air speed	0.1 <i>m/s</i>
Air relative humidity	40 %
Average heat capacity of human body	3470 J/(kg K)

Table 1 Initial assumptions for the analysis

3.3. Core and skin-layer temperatures: results and discussion

3.3.1 Case 1: $T_a = 21.5\text{ °C}$ and $T_{mr} = 23.5\text{ °C}$

In figure 9 is shown the trend of core and skin layer temperature during the transient. The two trends are represented in figures 10 and 11 more in detail. Skin layer temperature has a variation which agrees with the environmental conditions around the body. In this case the air temperature is sufficiently lower than the skin set point temperature to cause a drop of skin-layer temperature. The equilibrium of the skin with the surrounding conditions is reached after an exposure longer than 200 minutes.

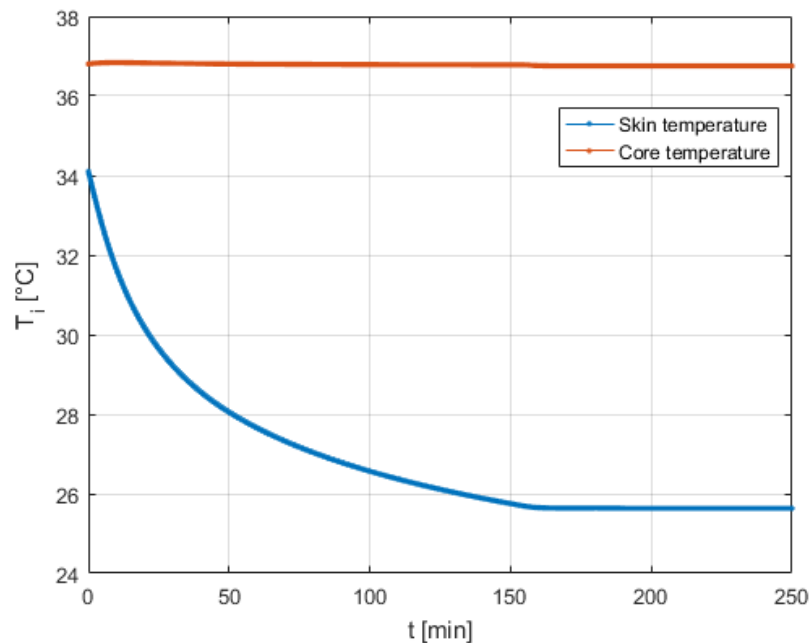


Figure 9. Core and skin temperature trend in time

Core temperature variation between the beginning and the end of the transient is lower than 0.04 °C , as it is noticeable from figure 10.

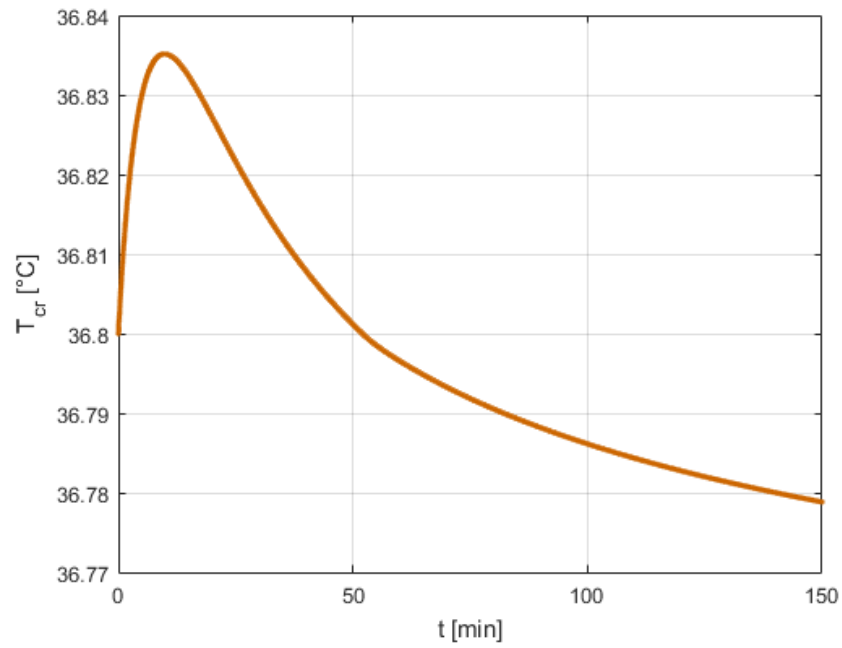


Figure 10. Core temperature trend

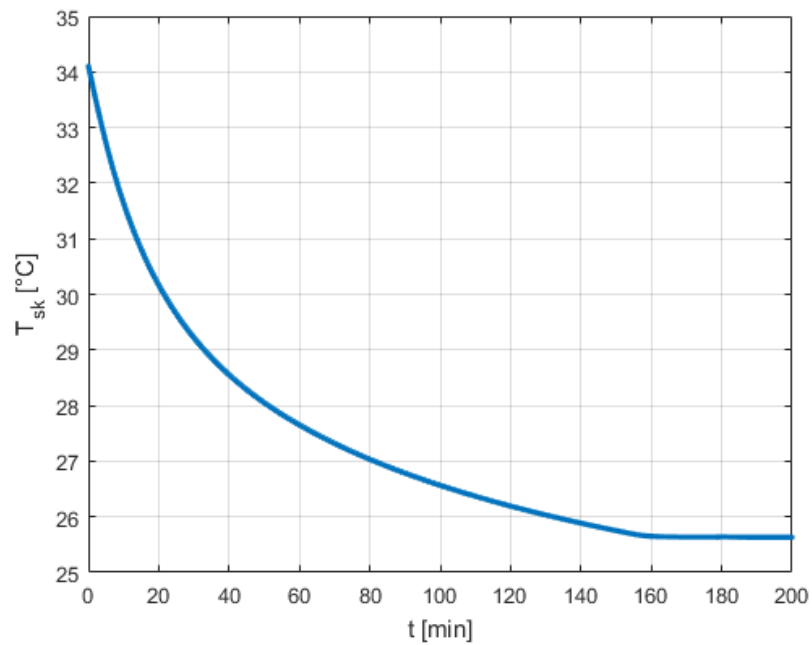


Figure 11. Skin temperature trend

Thermal interaction between core and skin compartments has been analysed and the variable representing this interaction has been so defined:

$$Q_{cr-sk} = K(T_{cr} - T_{sk}) \quad (3.8)$$

considering that the layers can exchange heat only through conduction.

The evaluation of this quantity during the transient turned out the result shown in figure 11.

As the temperature difference between core and skin decreases, the increase in heat transfer rate is less pronounced, till the two temperature become constant and Q_{cr-sk} stabilizes around 60 W/m^2 . Obviously, thermal transfer is never null because a temperature difference between core and skin always exists.

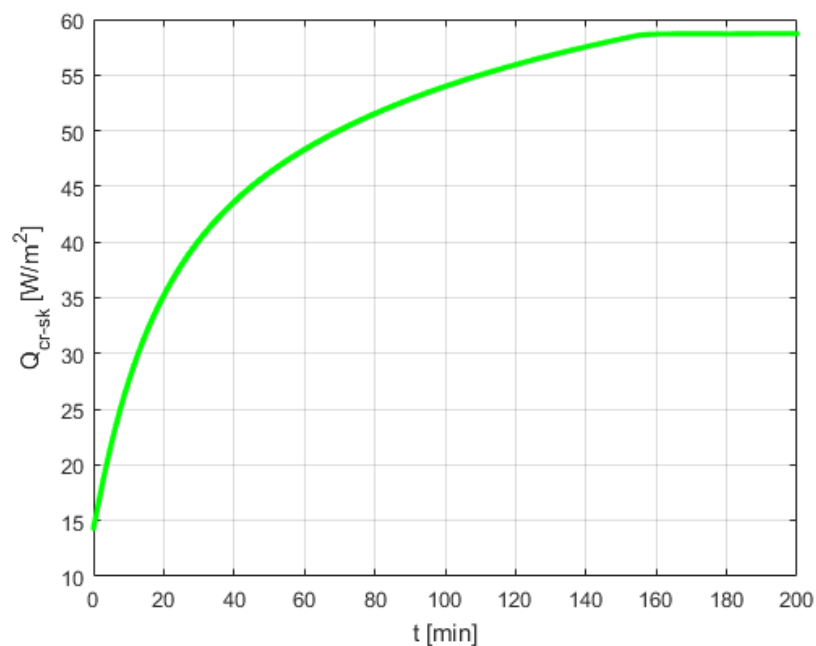


Figure 12. Heat transfer rate between core and skin in time

Other conditions have been analysed, in which we change the air temperature and the mean radiant temperature to see how the final core and skin temperatures vary and if the duration of the transient is affected.

In sections 3.3.2. and 3.3.3., two extreme situations have been considered, so that it is possible to see clearly the difference with respect to the previous case.

3.3.2. Case 2: $T_a = 7^\circ\text{C}$ and $T_{mr} = 5^\circ\text{C}$

Very low temperatures turned out very short transient with respect to the previous case. This time, skin and core temperature stabilize completely after less than 1 hour exposure to the described environment (figure 13)

Same considerations can be done for heat transfer between core and skin. It becomes stable after the same time interval and its final value is between 55 and 60 W/m^2 , but this time it increases quicker than before (figure 14).

It is interesting to notice that the value reached by heat transfer at the end of the transient is constant, whatever conditions we may have in the surrounding environment; in fact, if Q_{cr-sk} is computed using equation 3.8, it depends on the effective conductance between core and skin, which is constant and equal to 5.28 $\text{W}/(\text{m}^2\text{K})$.

Q_{cr-sk} initial value in both cases is equal to:

$$Q_{cr-sk}(t = 0) = K(T_{cr,set} - T_{sk,set}) = 5.28(36.8 - 34.1) = 14.256 \text{ W}/\text{m}^2 \quad (3.9)$$

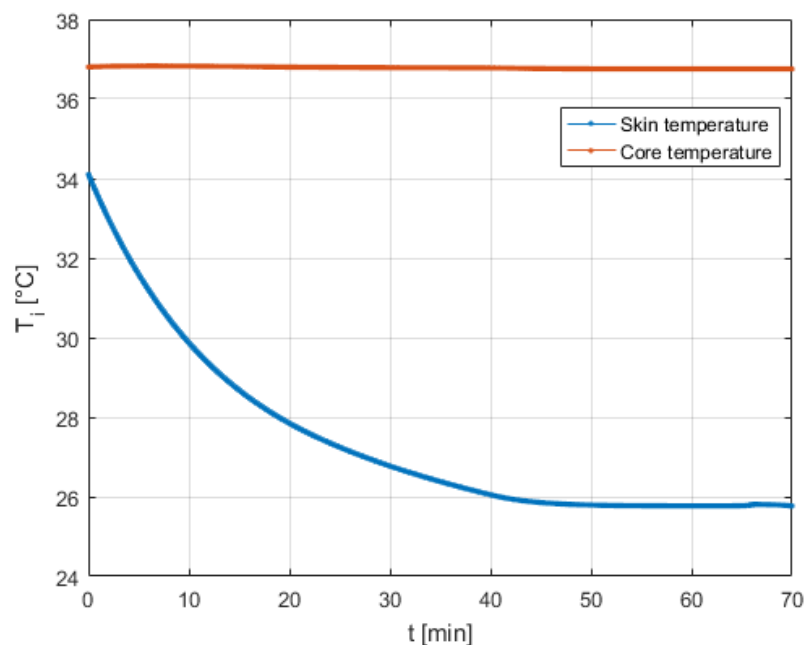


Figure 13. Core e skin temperature trend in time (case 2)

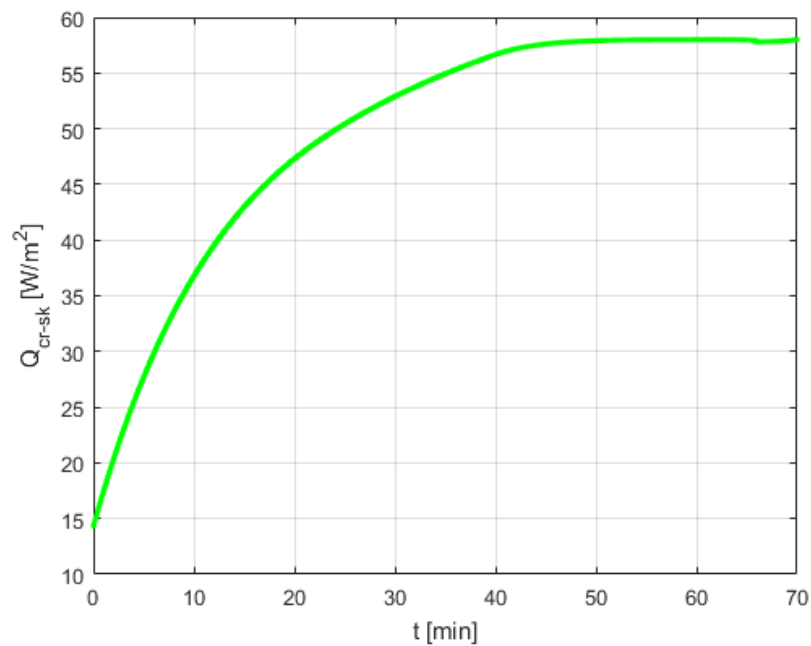


Figure 14. Heat transfer rate between core and skin in time

3.3.3. Case 3: $T_a = 34\text{ }^\circ\text{C}$ and $T_{mr} = 34\text{ }^\circ\text{C}$

In this case air temperature and mean radiant temperature are extremely high. The obtained results are shown in figures 15, 16 and 17.

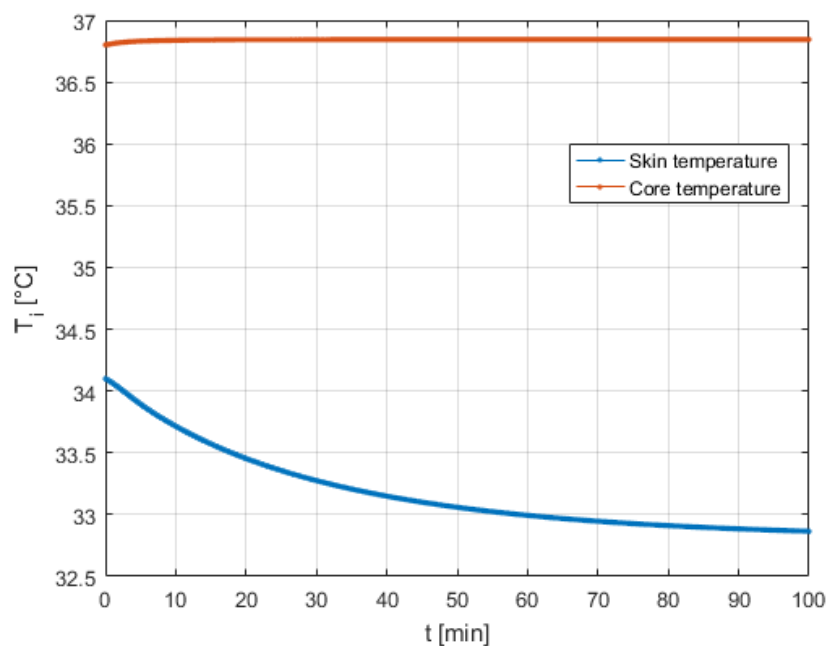


Figure 15. Core e skin temperature trend in time (case 3)

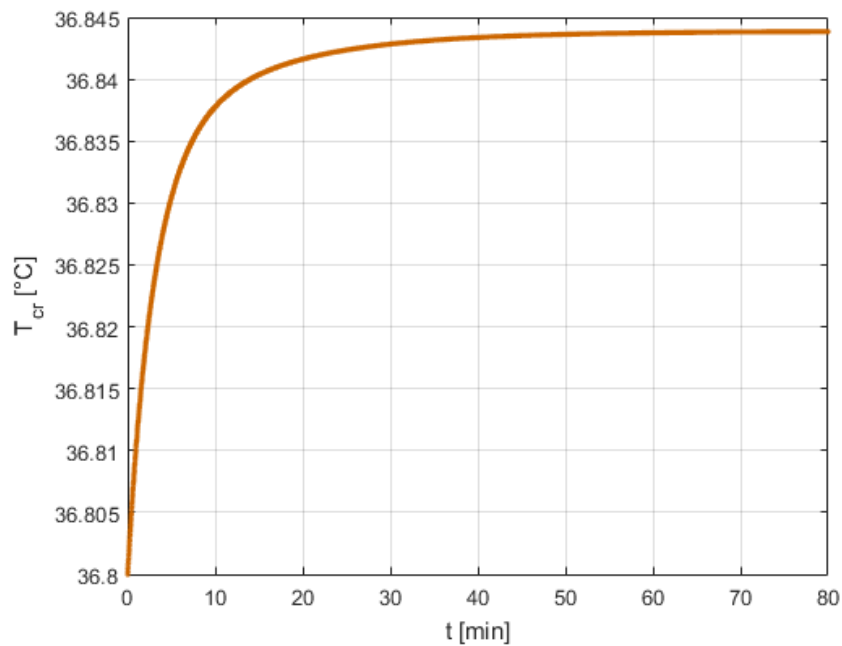


Figure 16. Core temperature trend

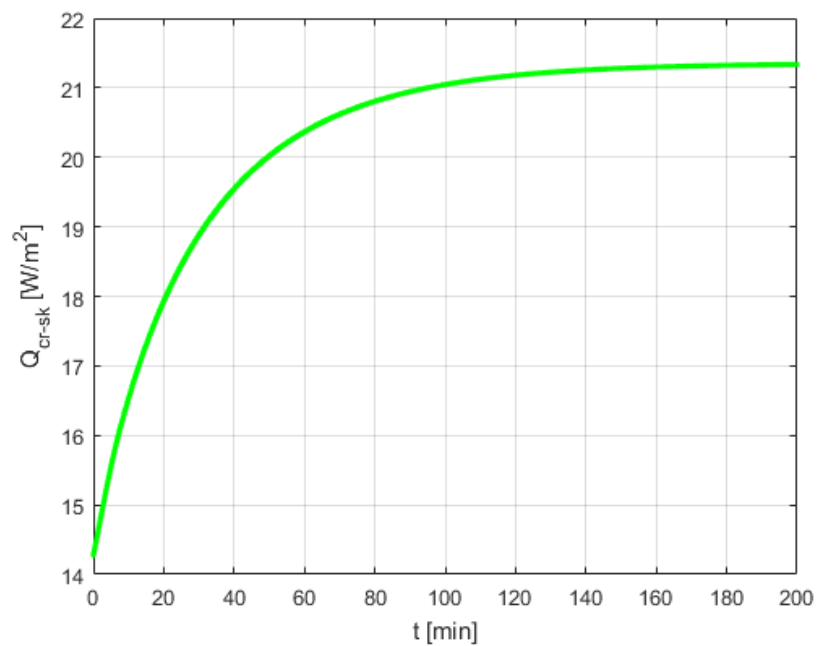


Figure 17. Heat transfer rate between core and skin in time

The transient has a duration comparable with the initial case; final skin-layer temperature rises up around 33 °C, due to the small temperature difference with the surrounding climate.

It is important to notice that core temperature is almost constant in all the considered cases. The reason to this trend has to be found in the presence of the thermoregulation processes characterizing the human body, which prevent this temperature from rising above 39 °C at which confusion, muscle cramps and often nausea or vomiting occurs as initial symptoms of hyperthermia.

3.4. Generalizations

Finally, it is possible to plot the trend of core temperature, skin-layer temperature and heat transfer between core and skin under constant air temperature and varying the mean radiant temperature, leaving the other variables unchanged.

In this last case, the air temperature has been chosen to be 20 °C, while mean radiant temperature has been changed from 15°C to 30 °C.

In general, it can be affirmed that a mean radiant temperature rising causes an increment in the final skin-layer temperature and in the duration of its transient (figure 18). Looking at the core temperature trend (figure 19), the same behaviour has been recorded, but the core temperature trend has a stronger dependency on air temperature.

To clarify this sentence, let us analyse figure 20, where air temperature has been set at 38 °C (very unlikely to happen in moderate environments) and mean radiant temperature has been changed from 30°C to 38 °C.

It is clearly noticeable that the increase of air temperature above 30 °C, turned out an opposite trend of core temperature. The human body system, preventing the abnormal increase of core temperature, causes the opposite effect.

Maybe this trend could depend on the increase of the sweat secretion rate.

In extremely hot climatic conditions, the only way the body discharges extra-heat in the surrounding environment is through sweat. Perhaps because of heat capacity of water is greater than the air one, core temperature drops faster.

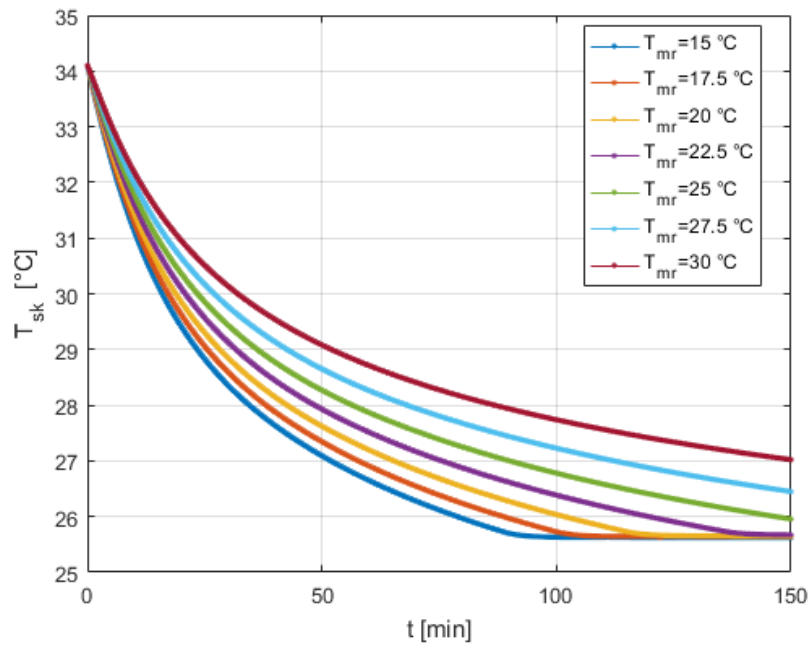


Figure 18. Skin-layer temperature trend with different mean radiant temperatures

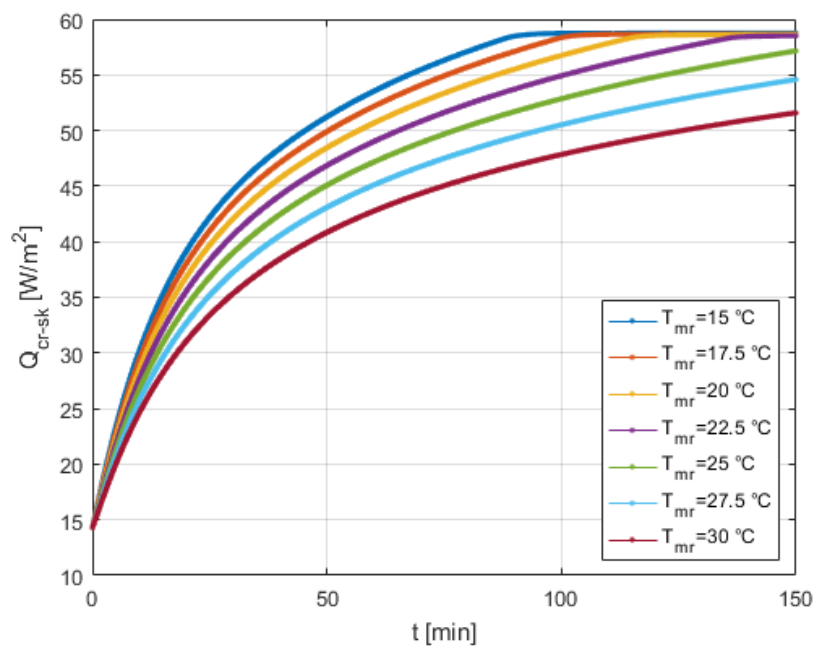


Figure 19. Heat transfer between core and skin with different mean radiant temperatures

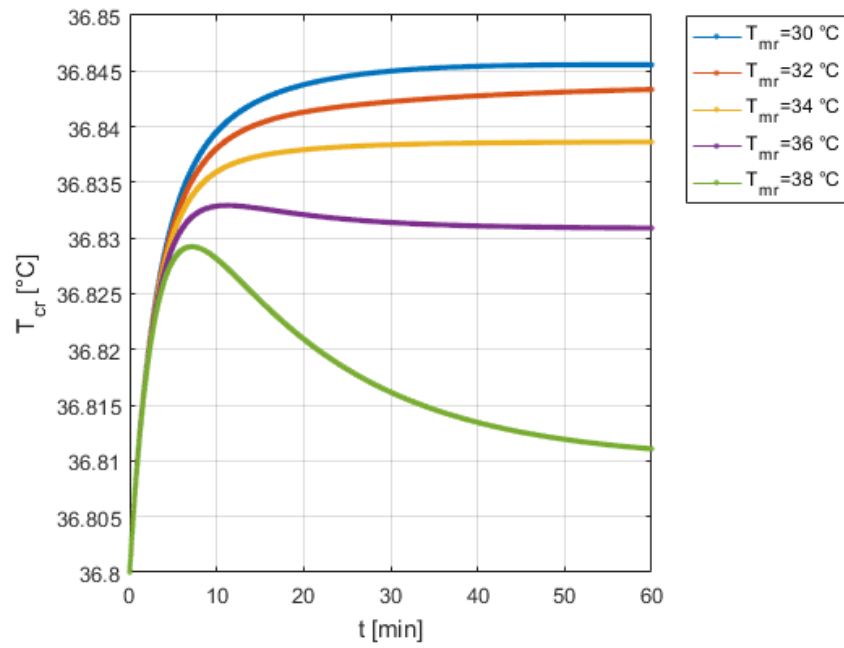


Figure 20. Core temperature trend with higher temperatures

4. Human body exergy efficiency

4.1. Exergy balance

From the thermodynamic point of view, the human body is an open system which operates using exergy-entropy processes [11]. There must be exergy balance for human body which is formally equivalent to the equation characterizing the energy balance (equation 2.1), but including one unique feature hence the term of “consumption”. Indeed, exergy is a conservative function for a reversible process only; all the natural phenomena are irreversible and characterized by a certain destruction of exergy, which corresponds to production of entropy.

Therefore, the general form of exergy balance equation for the system in question is as follows:

$$E_{x,in} - E_{x,destr} = E_{x,st} + E_{x,out} \quad (4.1)$$

being $E_{x,in}$, $E_{x,out}$, $E_{x,destr}$ and $E_{x,st}$ the exergy rate in input, the exergy rate in output, the exergy destruction rate and the total exergy storage rate respectively.

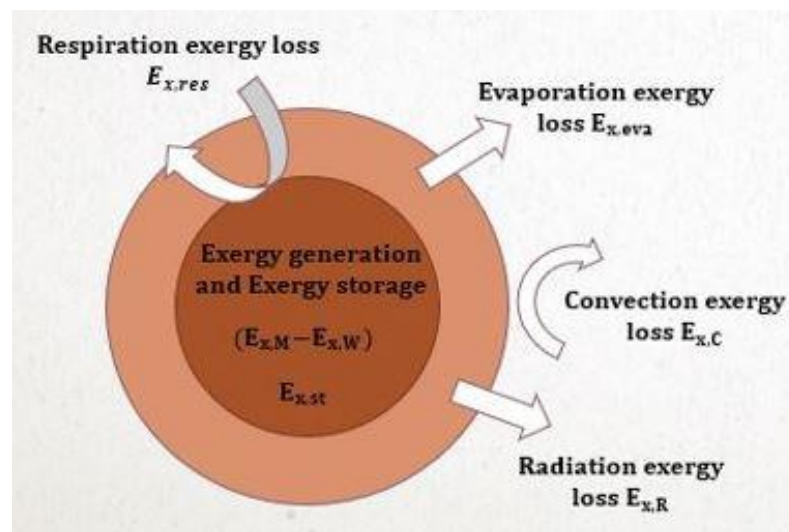


Figure 21. Exergy interaction between the human body and the surrounding environment [7]

Clarifying the meaning of each term of the previous equation:

$$(E_{x,M} - E_{x,W}) - E_{x,destr} = E_{x,st} + [E_{x,res} + (E_{x,eva} + E_{x,C} + E_{x,R})] \quad (4.2)$$

where:

$E_{x,M}$ is the metabolic exergy rate generated in the core compartment, related to the activity level;

$E_{x,W}$ is the mechanical exergy rate accomplished;

$E_{x,res}$ is the total exergy rate through respiration;

$E_{x,sk}$ is the total exergy rate from the skin through evaporation of sweat;

$E_{x,C}$ and $E_{x,R}$ are the sensible exergy rates due to convection and radiation respectively.

4.2. Exergy efficiency: definitions

Each term of equation 4.2 has been analysed from a mathematical point of view and it has been used for a proposal of a new efficiency index, which has been defined as:

$$\eta_{ex} = \frac{|E_{x,in} - E_{x,out} - E_{x,Mbas} - E_{x,st}|}{E_{x,in}} = 1 - \frac{|E_{x,out} + E_{x,Mbas} + E_{x,st}|}{E_{x,in}}$$

$$\eta_{ex} = 1 - \frac{|(E_{x,C} + E_{x,R} + E_{x,res} + E_{x,eva}) + E_{x,Mbas} + E_{x,st}|}{E_{x,in}} \quad (4.3)$$

The meaning of each term will be explained in the following sections.

4.2.1. Input exergy rate $E_{x,in}$

Daily caloric energy need for an average human, whose body mass is around 80 kg and who is tall around 180 cm, is around 2400 kcal [21].

The body area can be evaluated through Dubois' formula:

$$A_{body} = 0.007184 H^{0.725} M_{body}^{0.425} = 0.007184 * 180^{0.725} * 80^{0.425} = 1.9981 \text{ m}^2 \simeq 2 \text{ m}^2 \quad (4.4)$$

Knowing that 1 kcal is equivalent to 4186 J:

$$E_{in} = 2400 * 4186 = 10046.400 \text{ kJ} \quad (4.5)$$

$$e_{in} = \frac{E_{in}}{A_{Du}} = \frac{10046.4}{1.9981} = 5028 \frac{kJ}{m^2} \quad (4.6)$$

being e_{in} the specific energy in input per each square meter of body area.

The caloric energy need is defined as a daily quantity, so it is possible to find its value per each hour, considering that the input is constant in all the 24 hours of the day:

$$\dot{e}_{in} = \frac{e_{in}}{24} \frac{kJ}{m^2 h} = \frac{5028}{24 \cdot 3600} \frac{kJ}{m^2 s} = 58.194 \frac{J}{m^2 s} = 58.194 \frac{W}{m^2} \quad (4.7)$$

It has been assumed that all the energy in input coming from foodstuff, can be treated as pure exergy, hence:

$$E_{x,in} = \dot{e}_{in} \quad (4.8)$$

4.2.2. Exergy rate related to basal metabolism $E_{x,M_{bas}}$

Basal metabolism is expression of all the chemical reactions necessary to preserve the functional integrity of human body cells and tissues and to maintain body temperature constant [21]. It is defined as the energy expenditure of a human body in relaxed conditions, which is not performing any physical activity: in this conditions, basal metabolism represents the energy used for keeping active the vital functions (heartbeat, blood circulation, pulmonary dilatation, etc.).

It can be evaluated from the following formula:

$$E_{M_{bas}} = 11.6 M_b + 879 = 1826.7 \text{ kcal} \quad (4.9)$$

which turns out the result in [kcal]. Repeating the same calculation procedure done for E_{in} :

$$E_{M_{bas}} = 1826.7 * 4186 = 7646.65 \text{ kJ} \quad (4.10)$$

$$e_{M_{bas}} = \frac{E_{M_{bas}}}{A_{Du}} = 3826.96 \frac{kJ}{m^2} \quad (4.11)$$

$$\dot{e}_{M_{bas}} = \frac{e_{M_{bas}}}{24 \cdot 3600} = 44.293 \frac{W}{m^2} \quad (4.12)$$

Even this variable has been treated totally as available energy, so pure exergy.

4.2.3. Exergy storage rate $E_{x,st}$

The rate of heat storage in human body can be written taking into account two different contributions: heat storage rate in body core and in the skin-layer. In reality the heat is stored only in the body core and its value equals the rate of increase in internal energy. Therefore, we take separately these two rates only for mathematical simplicity and to have two different expressions each one dealing with the rate of change of core and skin-layer temperature.

Remembering equations 2.9 and 2.10:

$$Q_{cr} = (1 - \alpha_{sk}) \frac{M_{body}}{A_{Du}} c_{p,body} \quad (4.13)$$

$$Q_{sk} = \alpha_{sk} \frac{M_{body}}{A_{Du}} c_{p,body} \quad (4.14)$$

the total heat storage in human body can be expressed as the sum of these contributions and, considering that the heat is stored only in the body core, the exergy rate related to this process can be expressed as:

$$E_{x,st} = (Q_{cr} + Q_{sk}) \frac{[T_{cr}(n) - T_{cr}(n-1)]}{n\Delta t} \quad (4.15)$$

We must obtain a rate of energy per square meter of human body area. In fact, setting up the dimensional analysis (and ensuring that Δt is expressed in seconds):

$$[E_{x,st}] = \left[\frac{J}{m^2 K} * \frac{K}{s} \right] = \left[\frac{J}{m^2 s} \right] = \left[\frac{W}{m^2} \right] \quad (4.16)$$

The heat storage has been treated as overall available energy for human body, hence totally exergy.

4.2.4. Convective exergy transfer rate $E_{x,C}$

For a clothed person the sensible heat transfer through convection is determined as:

$$C = f_{cl} h_c (T_{cl} - T_a) \quad (4.17)$$

Therefore, the related exergy is expressed as:

$$E_{x,C} = C \left(1 - \frac{T_0}{T_{cl}} \right) = f_{cl} h_c (T_{cl} - T_a) \left(1 - \frac{T_0}{T_{cl}} \right) \quad (4.18)$$

The clothing temperature has been used to set up the expression because the human body is clothed; it is calculated using iteratively equation 2.31.

$\left(1 - \frac{T_0}{T_{cl}}\right)$ represents the Carnot factor, taking into account only the fraction of useful energy that could be effectively used as work and its value depends greatly on the chosen reference temperature T_0 .

4.2.5. Radiative exergy transfer rate $E_{x,R}$

The linearized radiant heat transfer coefficient is expressed through equation 2.29. The calculation of radiation exergy transfer rate has been taken from Wu [13]:

$$E_{x,R} = f_{cl} f_{eff} \varepsilon \sigma \left[(T_{cl}^4 - T_{mr}^4) - \frac{4}{3} T_a (T_{cl}^3 - T_{mr}^3) \right] \quad (4.19)$$

As all the other quantity appearing in the exergy balance, the unit of measure is $[W/m^2]$.

4.2.6. Respiration exergy transfer rate $E_{x,res}$

To express the exergy related to the mass transfer which occurs through respiration, first refer to the exergy of a mixture of ideal gases. Knowing the characteristics of each component, it is possible to calculate the exergy of the mixture per unity of mass as:

$$e_x = \sum_{i=1}^{ng} x_i * e_{x,i} \quad (4.20)$$

where x_i is the mass fraction of the i^{th} gas of the mixture, ng the total number of gases.

The exergy of each component has to be evaluated through the following relation:

$$\Delta e_x = h - h_0 - T_0(s - s_0) = c_p \left(T - T_0 - T_0 \ln \frac{T}{T_0} \right) + T_0 R^* \ln \frac{p}{p_0} \quad (4.21)$$

where h is the enthalpy and s is the entropy of the gas per unity of mass.

The subscript 0 refers to the gas characteristics at T_0 (reference temperature) and p_0 (reference pressure), while R^* is the gas specific constant in $[kJ/(kgK)]$ and c_p is the specific heat capacity at constant pressure in $[kJ/(kgK)]$.

Inhaled and exhaled air have been considered as a mixture of dry air and water vapour and both of them have been seen as ideal gases.

The air introduced into the human body through respiration is taken from the surrounding environment, hence it has the same humidity and temperature. On the

other hand, the exhaled air has different characteristics, it is warmer and its humidity is higher.

Using equation 4.20, the exergy related can be expressed as:

$$\Delta e_x = x_{dry} \Delta e_{x,dry} + x_{vap} \Delta e_{x,vap} \quad (4.22)$$

For dry air:

$$\Delta e_{x,dry} = c_{p,dry} \left(T_{cr} - T_0 - T_0 \ln \frac{T_{cr}}{T_0} \right) + T_0 R_{dry}^* \ln \frac{p_{dry}}{p_0} \quad (4.23)$$

where $c_{p,dry}$ is the heat capacity at constant pressure of the dry air, equal to 1005 J/(kgK) for temperatures between 20 °C and 40 °C; R_{dry}^* is the dry air specific constant (287.05 J/kgK), ratio of the universal constant of gases R (8.314 J/molK) and the molar mass of dry air (28.96 g/mol). The exhaled air has the same temperature as the core, because breathing is considered to happen at the core subsystem, while p_{dry} is the partial vapour pressure of the dry air in the overall exhaled air.

Similarly, for water vapour are valid the same considerations:

$$\Delta e_{x,vap} = c_{p,vap} \left(T_{cr} - T_0 - T_0 \ln \frac{T_{cr}}{T_0} \right) + T_0 R_{vap}^* \ln \frac{p_{vap}}{p_0} \quad (4.24)$$

$$\text{with } R_{vap}^* = \frac{R}{mm} = \frac{8314}{18.01528} \simeq 461.5 \frac{J}{kg K}$$

$$\text{and } c_{p,vap} = 1900 \frac{J}{kg K}$$

Dry air and water vapour partial vapour pressure can be evaluated following the procedure explained below.

According to Fanger [6] the mass flow rate of inhaled air can be estimated from:

$$m_{in} = (1.43 * 10^{-6}) q_{met} \quad (4.25)$$

The water vapour discharged from lungs and then delivered in the surrounding space by the exhaled air can be expressed as [22] [23]:

$$m_{vap,cr} = m_{in} (x_{ex} - x_{in}) \quad (4.26)$$

where x_{ex} is the mixing ratio of exhaled air and x_{in} is that of the surrounding air, so the inhaled air one. In other words, this variable represents the difference in vapour content between exhaled and inhaled air.

The mixing ratio x_{ex} can be estimated from:

$$x_{ex} = 2.77 * 10^{-2} + 0.65 * 10^{-4} T_a + 0.2 x_a \quad (4.27)$$

with T_a expressed in degree Celsius.

On the other hand, the mixing ratio of the surrounding air can be expressed as:

$$x_{in} = 0.622 \frac{p_a}{p} \quad (4.28)$$

where p_a is water vapour pressure at air temperature and p is the atmospheric pressure; their unity is Pascal.

Being $m_{vap,cr}$ the vapour mass discharged from lungs, the overall water vapour mass in the exhaled air is:

$$m_{vap,exh} = m_{vap,cr} + x_{in} m_{in} \quad (4.29)$$

and the overall dry air mass:

$$m_{dry,exh} = m_{in} - m_{vap,exh} \quad (4.30)$$

The mixing ratio of the exhaled air can be expressed as:

$$x_{vap,exh} = \frac{m_{vap,exh}}{m_{in}} \quad (4.31)$$

while

$$x_{dry,exh} = \frac{m_{dry,exh}}{m_{in}} = (1 - x_{vap,exh}) \quad (4.32)$$

Knowing these two values, the partial vapour pressure of dry air and water vapour are defined as:

$$p_{vap} = x_{vap,exh} * p_{cr} \quad (4.33)$$

$$p_{air} = x_{air} * p_{cr} = (1 - x_{vap}) p_{cr} \quad (4.34)$$

where p_{cr} is the saturation pressure at core temperature, x_{vap} is the mixing ratio of exhaled air.

Finally, applying equation 4.20, the exergy of the two components can be determined and the respiration exergy transfer rate has been estimated as:

$$E_{x,resp} = \frac{m_{in} \left[\frac{m_{vap,cr}}{m_{in}} \Delta e_{x,vap} + \left(1 - \frac{m_{vap,cr}}{m_{in}} \right) \Delta e_{x,dry} \right]}{n \Delta t} \quad (4.35)$$

4.2.7. Evaporation exergy transfer rate $E_{x,eva}$

The mass rate of water vapour evaporating from the skin surface has been calculated as:

$$m_{vap,sk} = \frac{w E_{max}}{10^3 r A_{Du}} \quad (4.36)$$

where w is the skin wetness factor, defined in equation 2.17 and E_{max} is the maximum rate of evaporation through human body, given by equation 2.21; r is the mean latent-heat of evaporation of liquid water for temperatures around 30 °C, whose value is 2450 kJ/kg. The unity of $m_{vap,sk}$ is [kg/s/m²].

The thermal power absorbed from the surrounding environment is then:

$$q_{eva} = m_{vap,sk} * r \quad (4.37)$$

and its unity is [kW/m²].

Therefore, the evaporation exergy transfer rate results to be:

$$E_{x,eva} = q_{eva} \left(1 - \frac{T_0}{T_a}\right) = m_{vap,sk} * r \left(1 - \frac{T_0}{T_a}\right) \quad (4.38)$$

and the Carnot factor is calculated using the air temperature because q_{eva} is exchanged with the surrounding environment.

4.3. Reference temperature

The calculation of exergy transfer rates needs the assumption of the reference temperature.

The choice of reference temperature is arbitrary, but it has to be done consistently with the characteristics of the system the analysis has to deal with.

Indeed, if the 'exergetic level' of the system is lower than the reference one, negative exergy comes out and it represents a physical nonsense.

To choose our reference characteristics it has been considered that our overall system (human body + environment) is other than the reference ambient, which has been assumed to have a temperature T_0 of 288 K (15 °C) and a reference pressure p_0 equal to atmospheric pressure, hence 101325 Pa.

There is no common agreement for a correct choice of reference environment. What has been noticed is that the system is more sensitive to the choice of the reference state when its conditions are near to the reference ones [24].

4.4. Exergy efficiency: results and discussion

The new exergy efficiency index has been analysed looking at how its value has changed modifying the boundary conditions of our problem.

Initially it has been studied the trend of this index as a function of time and the result obtained is shown in figure 22. All the thermal characteristics of the environment and the human body system are summarized in table 2.

While body core and skin-layer temperature reach their stabilized value, exergy efficiency index increases, till a maximum that, in this case, is around 24 %.

It is worthy to notice that the transient has a very short duration and exergy efficiency achieves its final value in less than 5 minutes. Therefore, it is not wrong to assume that the human body response to an external stress is very rapid and that in few minutes the body system starts working with the highest efficiency to reach comfort conditions quickly.

	<i>Value</i>
Air temperature	22.5 °C
Mean radiant temperature	25 °C
Reference temperature	20 °C
Metabolism	1.1 <i>Met</i>
Clothing insulation	0.7 <i>clo</i>
Air speed	0.1 <i>m/s</i>
Air relative humidity	37 %
Average specific heat of human body	3470 <i>J/(kg K)</i>

Table 2 Initial assumptions for exergy analysis

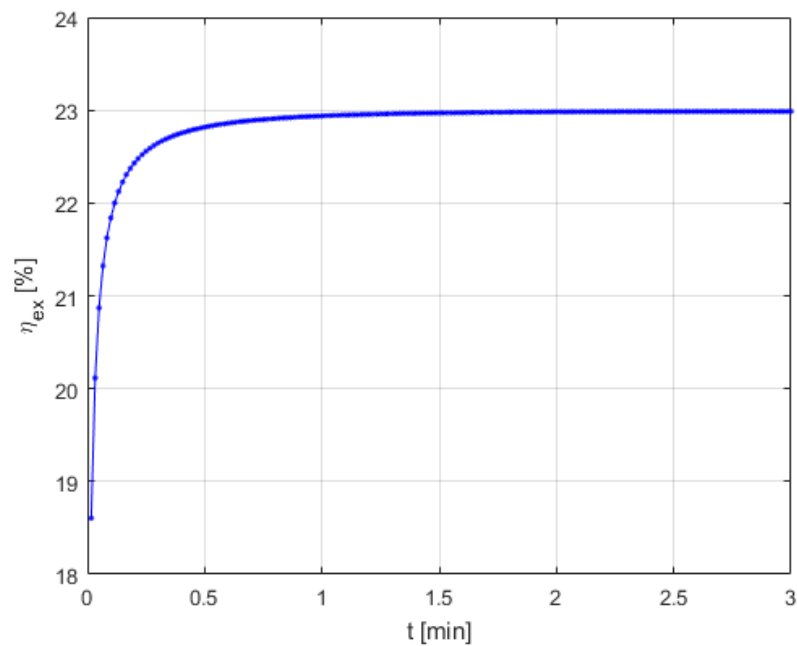


Figure 22. Human body exergy efficiency in time

Looking at the definition of η_{ex} (equation 4.3), clearly it depends on the exergy rates related to the energy transfers with the surrounding environment mainly by convection, radiation and evaporation. The trend of these functions over time has been plotted in figure 23.

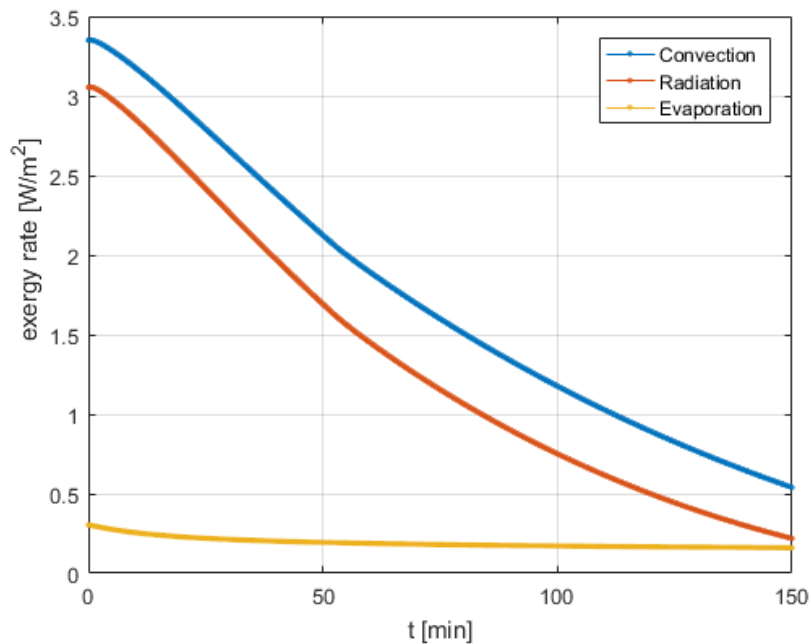


Figure 23. Convection, radiation and evaporation exergy rate on time

4.5. Exergy efficiency variation with different mean radiant and air temperatures

In figure 24 is shown the dependency of exergy efficiency from mean radiant temperature and fixing the air temperature at 22.5 °C.

Exergy efficiency index depends on mean radiant temperature and its value is greater when T_{mr} is smaller. However, the proportionality is not direct and the index increases less as much as the mean radiant temperature is low. Theoretically, the more the human body is in disequilibrium with the surrounding environment, the more the exergetic level increases; thus, the results seem to be in agreement with this statement.

The proportionality between air temperature and exergy efficiency (figure 25) seems to be more uniform with respect to the previous case. The decrease in air temperature of 2.5 °C causes an increment of the efficiency almost constant, independently on the value assumed by T_a .

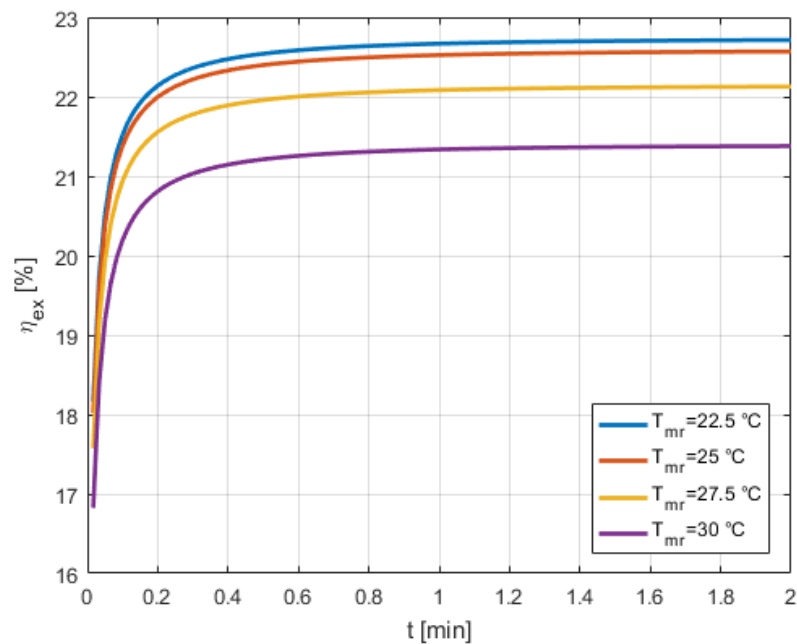


Figure 24. Exergy efficiency in time with different mean radiant temperatures

It is interesting to notice that the efficiency is higher when mean radiant temperature is higher than air temperature. In fact, when $T_{mr} = 22.5$ °C and $T_a = 25$ °C (figure 25), the

efficiency achieves value around 22 %, while when the situation is reversed efficiency stabilizes around 22.7 % (figure 24). The reason could be found in the variation of radiation exergy transfer rate, which influence the efficiency more than the convective one.

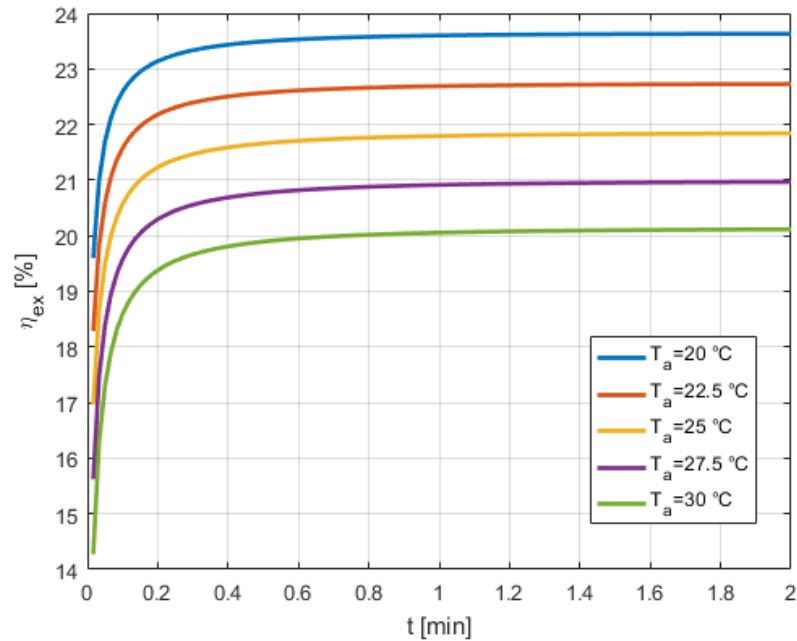


Figure 25. Exergy efficiency in time with different air temperatures

4.6. Exergy efficiency trend according to radiative and convective heat transfer coefficients

Exergy efficiency index has been tested for different value of radiative heat transfer coefficient and its trend is shown in figure 26.

It can be noticed that the variation of radiative heat transfer coefficient does not influence strongly the final value of exergy efficiency, but its contribution affects mainly the way in which the transient evolves. In particular, the highest is the radiative heat transfer coefficient, the more quickly efficiency reaches its final value.

Regarding the final values reached by η_{ex} , figure 27 shows the exergy efficiencies when the end of the transient occurs for all the considered curves. The result is consistent with the logic that higher h_r means higher radiative heat transfer rate and thus higher exergy

destruction during the heat transfer process. The latter appears with negative sign in the mathematical definition of η_{ex} , therefore the efficiency rises with a reduction of the radiative heat transfer coefficient. Indeed, the efficiency transient characterized by higher radiative heat transfer coefficient ends up in a shorter time interval.

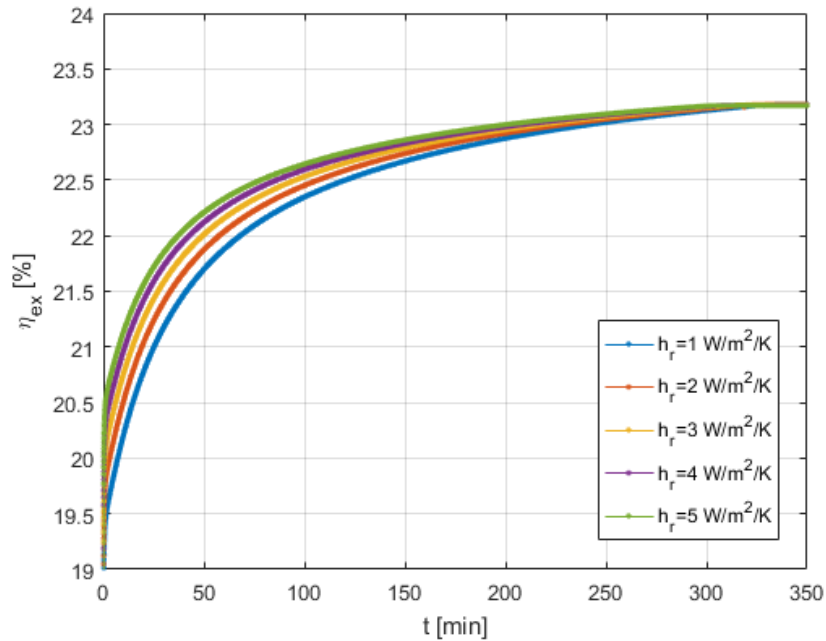


Figure 26. Exergy efficiency with different radiation heat transfer coefficients

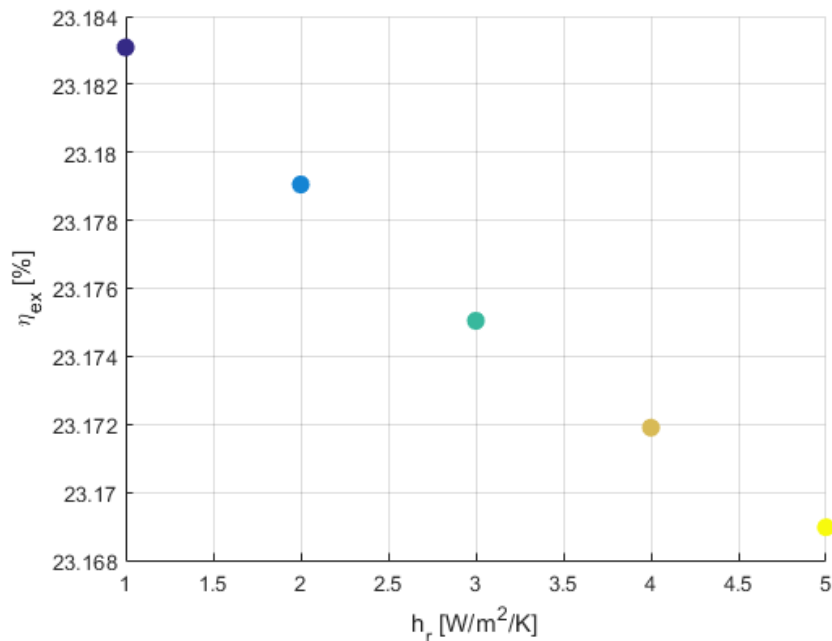


Figure 27. Final values of exergy efficiency as function of radiative heat transfer coefficient

The relationship between exergy efficiency and convective heat transfer coefficient is similar (figures 28 and 29). Even in this case, the reduction of exergy performance is caused by an increment of h_c and this trend is constant from the beginning till the end of the transient, unlike what happened according to radiative heat transfer coefficient.

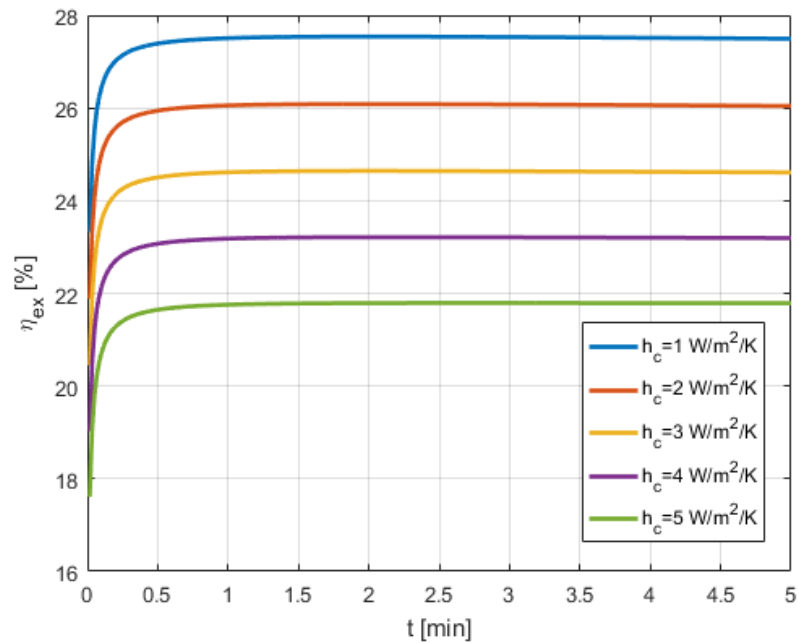


Figure 28. Exergy efficiency with different convective heat transfer coefficients

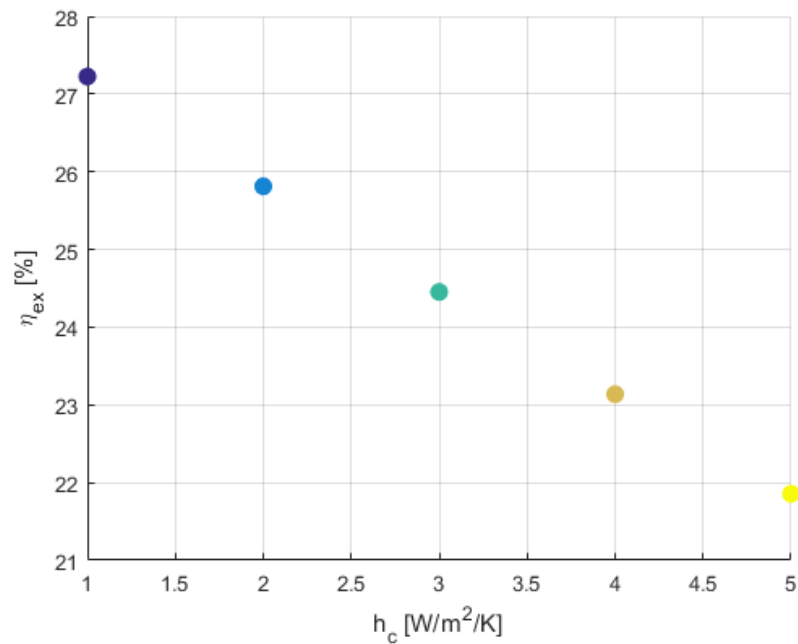


Figure 29. Final values of exergy efficiency as function of convective heat transfer coefficient

4.7. Exergy efficiency and environment temperatures

The relation between exergy efficiency, mean radiant temperature and air temperature is displayed in figure 30. In the plot is shown the final value reached by exergy efficiency, that has been taken as a new variable worthy of analysis.

It is clear that (for the considered personal and environmental factors), the maximum efficiency is reached only with certain combinations of air temperature and mean radiant temperature. At much lower air or mean radiant temperature, the exergy rate due to shivering causes lower exergy efficiency values, because it increases the exergy consumption. In the same way when the environment becomes hotter, sweating takes place and its presence causes the same effect.

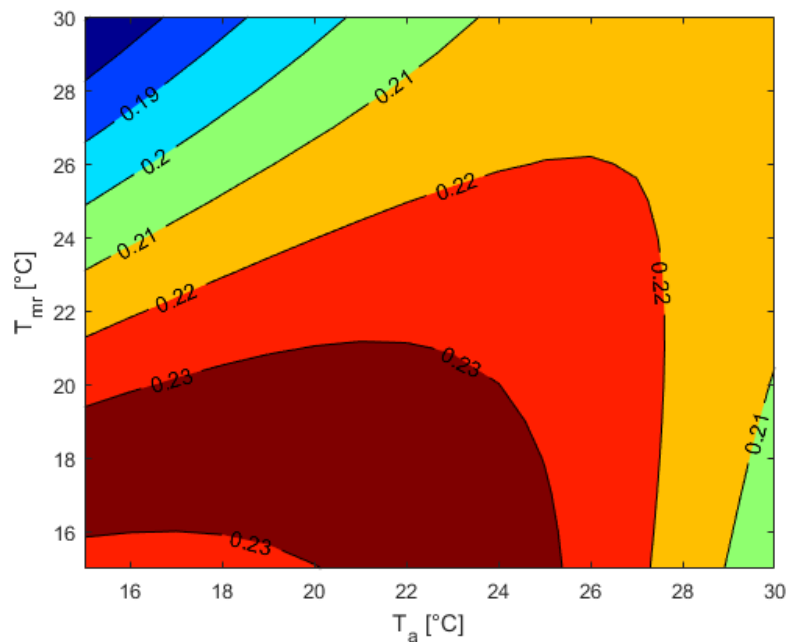


Figure 30. Exergy efficiency as a function of both mean radiant and air temperatures

Moreover, the occurrence of a maximum value indicates that there may be a relationship between exergy efficiency and the expected level of thermal comfort.

Figure 31 is a 3D plot of exergy efficiency again as a function of mean radiant and air temperature. It is clear that, in this case, efficiency varies from a maximum of 0.23 till the minimum values around 0.18. In general, we can state that its values are below 30

% (with the assumed personal and environmental parameters), so that around 70 % of the exergy in input is destroyed for in the energy and mass transfer processes and through basal metabolism.

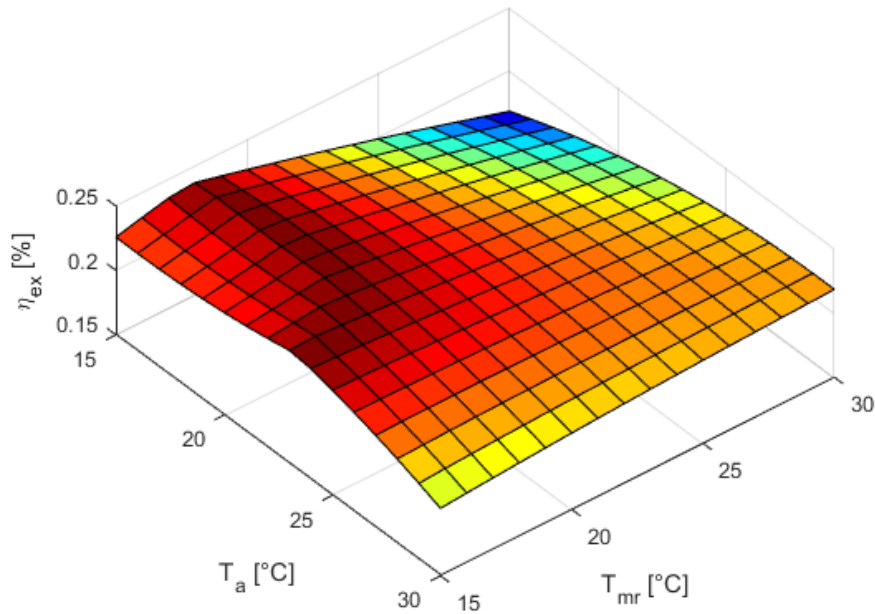


Figure 31. 3D plot of exergy efficiency as a function of both mean radiant and air temperatures

4.8. Exergy efficiency and mean air velocity

It has been analysed the response of the simulation to a different values of mean air velocity, to test how it affects the efficiency distribution (figure 32 and 33).

Variation of air speed influences the value of convective heat transfer coefficient, hence exergy destruction due to convection heat transfer.

Relatively small variation of air velocity causes a high change in efficiency distribution.

When the air velocity decreases, the maximum efficiency moves towards higher temperatures. Moreover, in case of higher v_{air} and moving towards higher temperatures (figure 33), mean radiant and air temperature have the same influence on exergy efficiency and its distribution becomes more uniform. As instance, taken $T_a = 24$ °C and $T_{mr} = 28$ °C, the efficiency results to be around 0.2. If temperature values are exchanged, the same efficiency is reached.

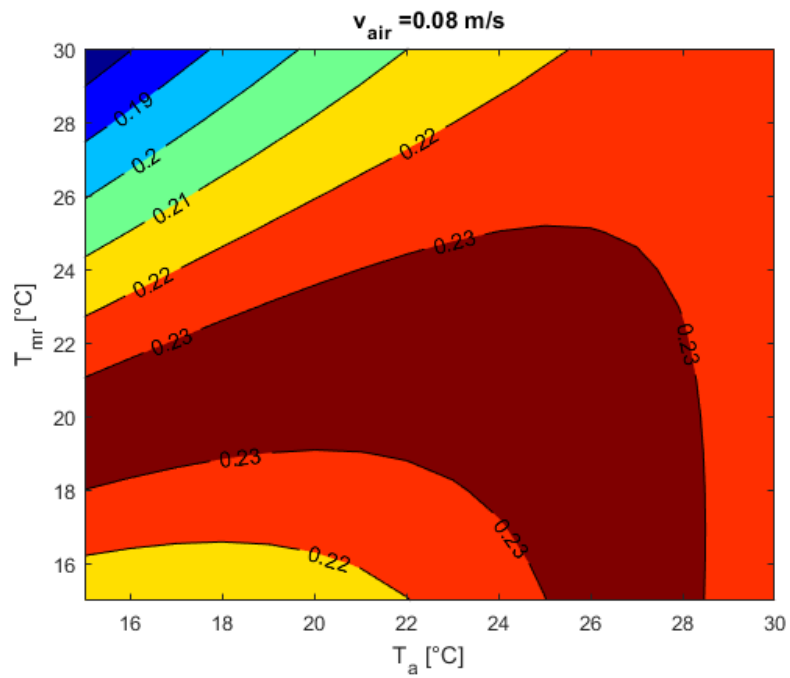


Figure 32. Exergy efficiency variation with $v_{air} = 0.08$ m/s

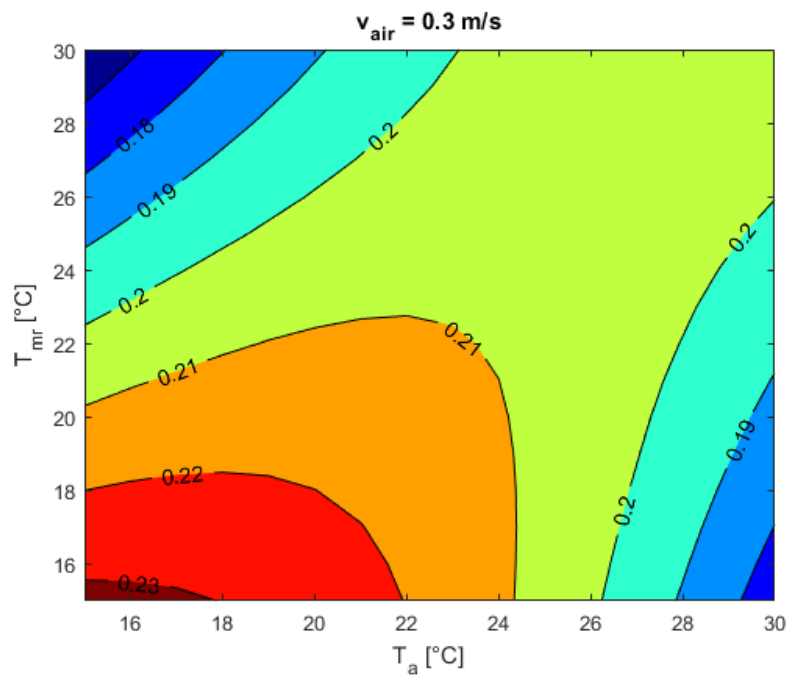


Figure 33. Exergy efficiency variation with $v_{air} = 0.3$ m/s

5. Exergy efficiency and thermal comfort

5.1. PMV trend

The energetic definition of comfort states that “the state of thermal comfort is reached when the heat flows to and from the human body are balanced and the skin temperature and sweat rate are in comfort range” [16]. For this purpose, Predicted Mean Vote model has been used.

The aim of the following sections is to verify the existence of a correlation between exergy efficiency and PMV index and to assess if exergy efficiency could be a useful indicator of thermal comfort.

PMV has been evaluated through the following calculation:

$$PMV = (0.303e^{-0.036M} + 0.028)[(M - W) - C - R - E_{sk} - C_{res} - E_{res}] \quad (5.1)$$

where the symbols have the meaning explained in the second chapter (section 2.2).

Convective and radiative heat transfer have been found from the equations below:

$$C = f_{cl}h_c(T_{cl} - T_a) \quad (5.2)$$

$$R = \varepsilon\sigma f_{cl}f_{eff}(T_{cl}^4 - T_{mr}^4) \quad (5.3)$$

E_{sk} represents the evaporative heat exchange through skin in neutral conditions and it has been calculated as:

$$E_{sk} = w * E_{max} = wF_{pcl}f_{cl}I_r h_c [p_{sks}(T_{sk,set}) - p_a(T_a)] \quad (5.4)$$

The trend of PMV has been analysed using the same personal and environmental parameters as for exergy efficiency analysis (section 4.4. – table 2).

For the specified conditions, PMV starts from an initial value of -1 and rises till a stabilized value around 1.5. The plot shows the PMV trend after the exposure in the new environment, but it is not giving any information about the transition from the neutral initial condition (PMV = 0) till the value of -1. Therefore, this part of the model is valid only in this time range, being unknown what happened during the first time step.

Moreover, values above 3 and lower than -3 have been voluntary cut, to take into account the real PMV variation range.

For different mean radiant temperatures, PMV has the trend shown in figure 35.

Obviously, the analysis has turned out higher PMV values when mean radiant temperature rises. The result is clearly shown in figure 36, where the final PMV values have been plotted as function of T_{mr} .

To be in thermal comfort condition ($-0.5 \leq PMV \leq +0.5$), mean radiant temperature has to vary in the interval $15 \text{ °C} \leq T_{mr} \leq 22.5 \text{ °C}$, according to personal and environmental parameters assumed in this part of the analysis.

It has been plotted PMV as a function of mean radiant and air temperature and the outcome is shown in figure 37. PMV trend is in agreement with the results obtained by Prek, Mazej and Butala in their research [16] and it confirms the strong PMV dependency on T_a and T_{mr} .

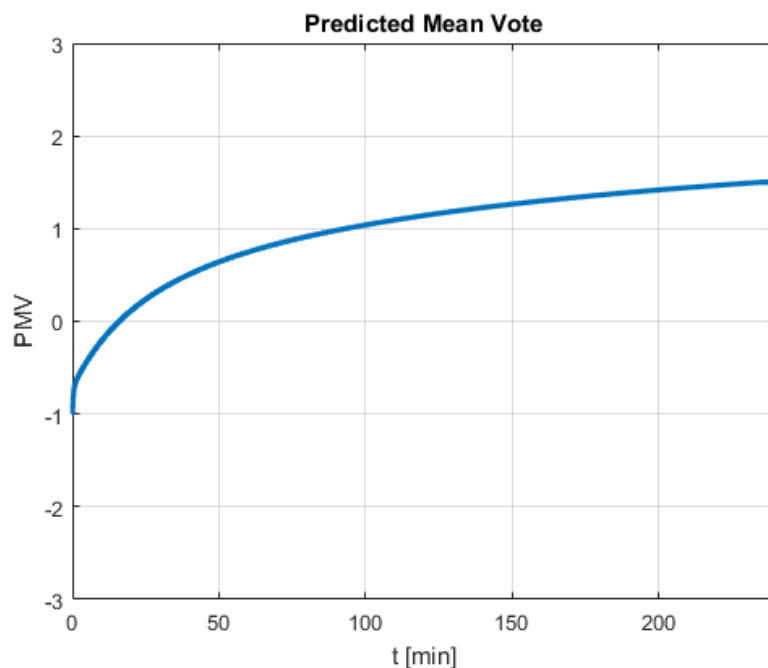


Figure 34. PMV trend in time

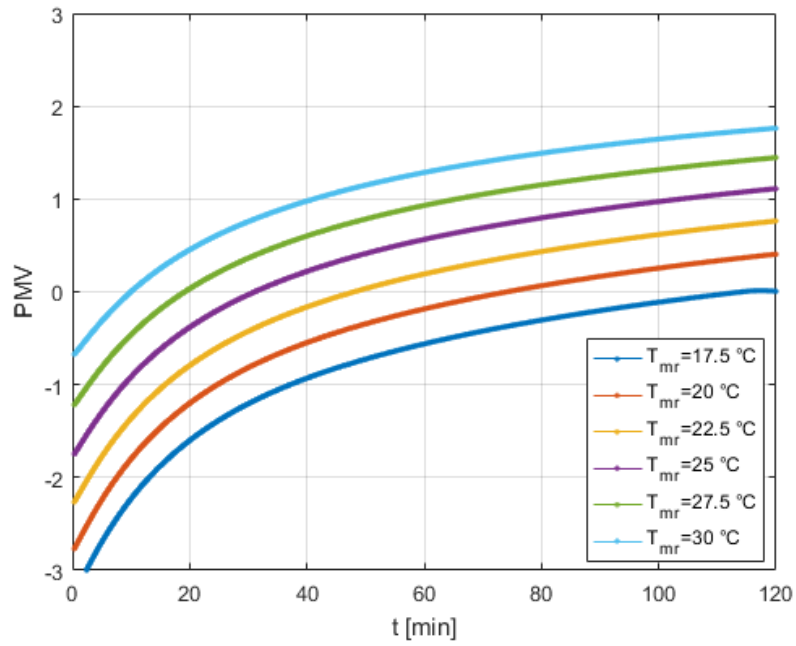


Figure 35. PMV trend with different mean radiant temperatures

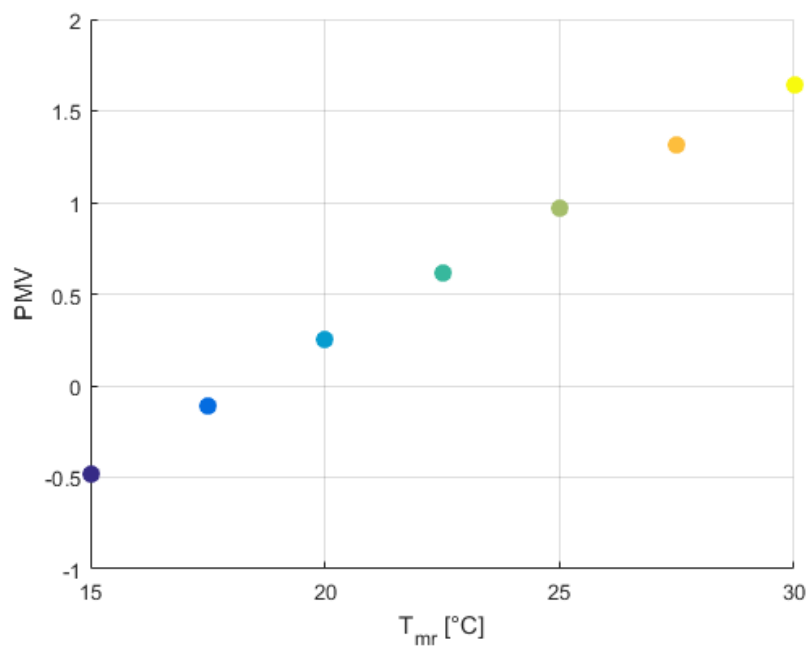


Figure 36. Final PMV values with different mean radiant temperatures

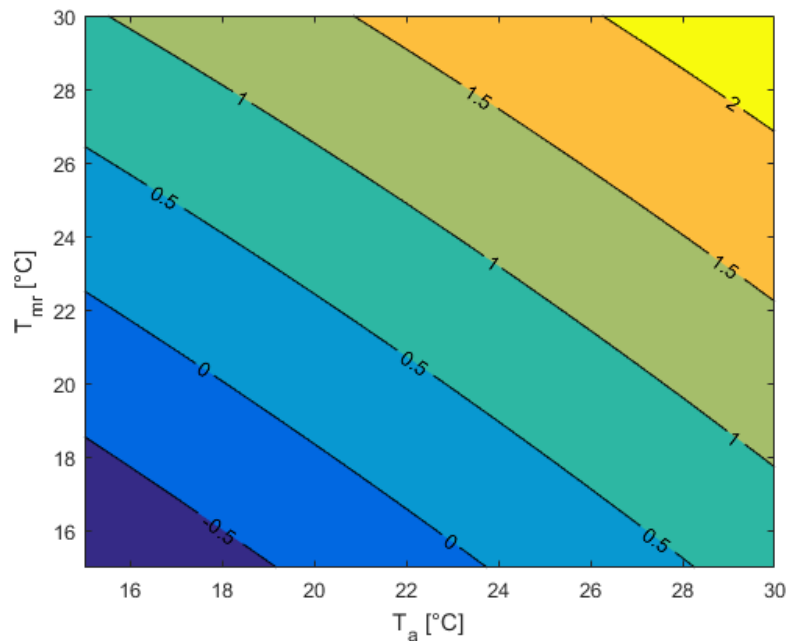


Figure 37. PMV as a function of both mean radiant and air temperatures

5.2. Exergy and PMV

The relationship between PMV and exergy efficiency can be visualized from figure 38, where the two variables have been represented together as functions of mean radiant temperature and air temperature.

As already has been explained in chapter 1, in the previous researches PMV had been correlated with exergy consumption and such analyses indicated that the minimum exergy consumption coincides with a neutral thermal sensation, in particular within the 'slightly cool-neutral' interval.

In this case, PMV and exergy efficiency areas are rather overlapped: in particular, where the exergy efficiency is at the maximum value, we find neutral thermal conditions or at most 'slightly-cool' thermal sensations. Exergy efficiency drops both towards positive and negative PMV values, hence it becomes smaller when we move far from thermal neutrality.

For the assumed environmental and personal parameters, the combinations of mean radiant and air temperatures which assure neutral or pleasant sensation are limited.

It is interesting to notice that, at higher temperatures, efficiency is much bigger when mean radiant temperature is lower than air temperature. Moreover, when higher mean radiant temperatures occur, a small change in air temperature causes a quick drop of efficiency; on the contrary, this effect is almost negligible when the situation is reversed and the environment is characterized by high air temperature.

Regarding thermal comfort, while it is true that where the exergy efficiency is at the maximum value, we find neutral thermal sensations, it is not true the contrary statement. In fact, PMV could be within (-0.5, 0.5) range even with lower efficiencies. It is noteworthy that, when efficiency is not at its maximum but thermal comfort occurs, mean air temperature result to be always lower (or at most equal) than mean radiant temperature.

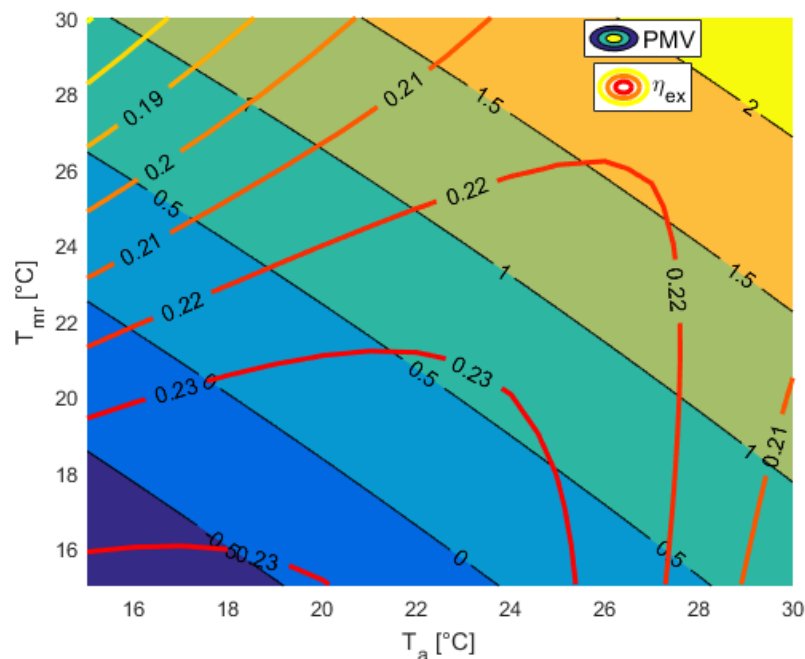


Figure 38. PMV and exergy efficiency

As an example, in figure 39 the variation of exergy efficiency considering air temperature equal to 20 °C and changing mean radiant temperature is shown. Each point of the curve can be seen as a particular combination (T_a, T_{mr}) , with fixed relative humidity.

The maximum efficiency in the considered case is reached when mean radiant temperature is 21 °C and in the same point, PMV results to be around zero.

For different air temperatures, the result is represented in figure 40.

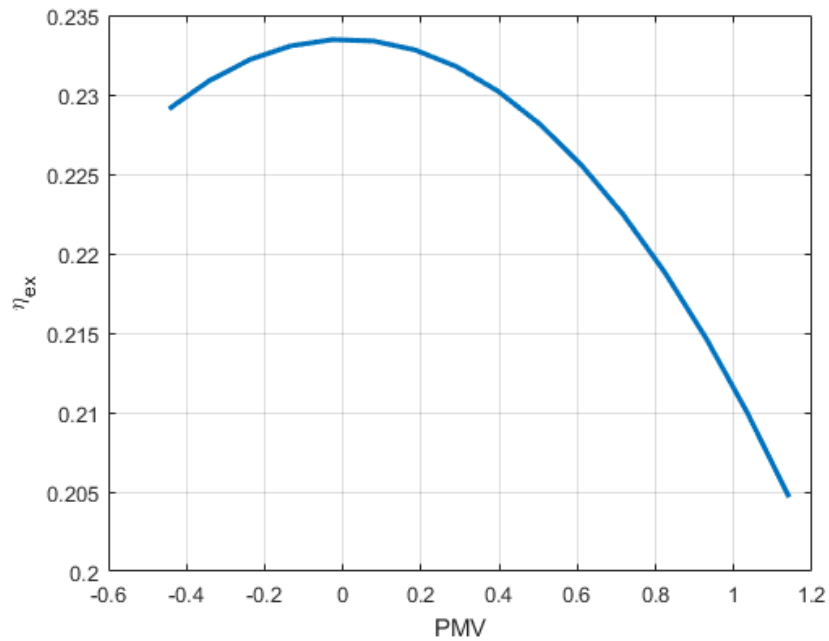


Figure 39. Exergy efficiency as a function of PMV

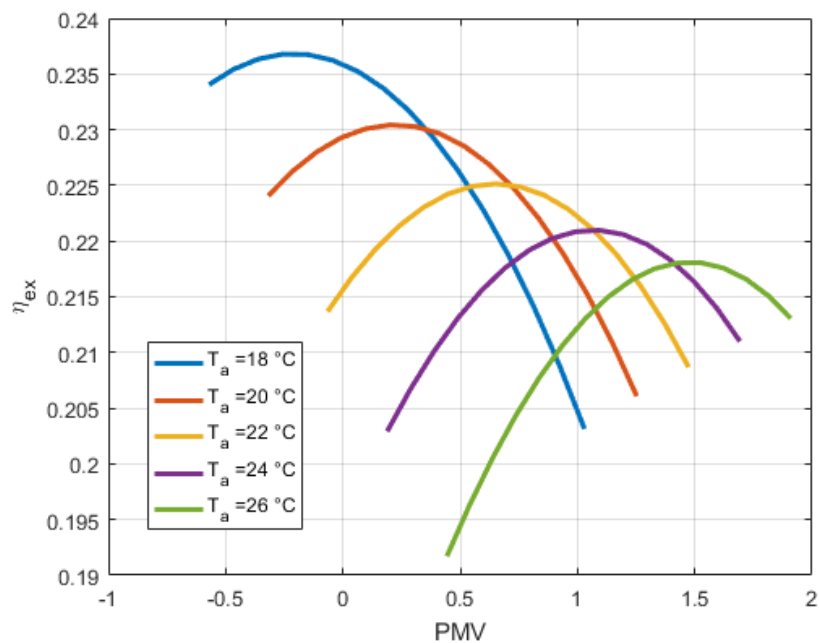


Figure 40. Exergy efficiency as a function of PMV for different air temperatures

After many simulations it has been understood that the exergy model is valid and it turns out logical results with assumed temperature from 10 °C to 34 °C, hence in moderate environments.

5.3. Sensitivity analysis on f_{eff}

5.3.1. Calculation of f_{eff}

In the analysis, the effective radiation area factor f_{eff} has been chosen accordingly with the existing literature. Many authors gave it values around 0.7 or 0.8 and in this section, will be tried to understand where these values come from and how they affect the exergy balance.

The effective radiation area factor has been experimentally determined by many research engineers for both standing and seated subjects, with very discrepant results. Fanger [6] proposed the analytical basis giving a mathematical explanation to the data found by experiments and measurements.

Following the procedure described by Fanger, let us consider a person located in the centre of a sphere, where in spherical coordinates it is possible to define the exact position of the person through the azimuth angle α and the altitude angle β . The reciprocity theorem of angle factors is valid and through it:

$$A_{eff}F_{p-A_2} = A_2F_{A_2-p} \quad (5.5)$$

where:

A_{eff} is the effective radiation area of the person;

F_{p-A_2} is the angle factor between the person and the sphere (A_2);

A_2 is the area of the sphere ($A_2 = 4\pi r_m^2$);

F_{A_2-p} is the angle factor between the sphere and the person.

If F_{p-A_2} represents the fraction of radiation that leaves the person and arrives at sphere surface, it is obvious that it is equal to one. So:

$$A_{eff} = 4\pi r_m^2 F_{A_2-p} \quad (5.6)$$

To estimate the angle factor F_{A_2-p} , it has to be considered a differential surface element dA_2 on the sphere, with coordinates (α, β) . The angle factor between dA_2 and the person then is:

$$F_{dA_2-p} = \frac{A_p}{\pi r_m^2} \quad (5.7)$$

with A_p that is the person's projected area on a plane to the direction of dA_2 .

Then, equation 5.7 becomes:

$$F_{A_2-p} = \frac{1}{A_2} \int_{A_2} \frac{A_p}{\pi r_m^2} dA_2 \quad (5.8)$$

Considering that $A_2 = 4\pi r_m^2$ and $dA_2 = r_m d\alpha r_m \cos\beta d\beta$:

$$F_{A_2-p} = \frac{1}{4\pi^2 r_m^2} \int_{\alpha=0}^{\alpha=2\pi} \int_{\beta=-\frac{\pi}{2}}^{\beta=\frac{\pi}{2}} A_p \cos\beta d\alpha d\beta \quad (5.9)$$

Since the human body is symmetrical and A_p is equal for two any opposite directions, the extreme of the integrals could be changed if we multiply them for the factor 4:

$$F_{A_2-p} = \frac{1}{\pi^2 r_m^2} \int_{\alpha=0}^{\alpha=\pi} \int_{\beta=0}^{\beta=\frac{\pi}{2}} A_p \cos\beta d\alpha d\beta \quad (5.10)$$

Returning to equation 5.6 and substituting F_{A_2-p} :

$$A_{eff} = \frac{4}{\pi} \int_{\alpha=0}^{\alpha=\pi} \int_{\beta=0}^{\beta=\frac{\pi}{2}} A_p \cos\beta d\alpha d\beta \quad (5.11)$$

If the exact position of the body is known, then α and β are known, while A_p values had been experimentally determined, considering 78 different angles within a quarter of sphere. The values that had been observed, have to be then interpolated, to find a single A_p value. Finally, for a nude person, the effective radiation area factor is:

$$f_{eff} = \frac{A_{eff}}{A_{Du}} \quad (5.12)$$

5.3.2. Influence of f_{eff} on exergy comfort model

f_{eff} takes into account of radiation angle factor between different body parts, which see each other's. Because of the human body has been considered to have the same temperature on the skin-layer/clothed surface, these contributions are null and they do not influence the exergy balance.

In figure 41 we can visualize how much a different effective radiation area factor could influence the radiation exergy rate, considering four different f_{eff} ; higher radiation area factors mean higher initial radiation exergy rate and greater pendency of the curves.

Radiation heat transfer coefficient is a linear function of effective radiation area factor (Table 3), as expected.

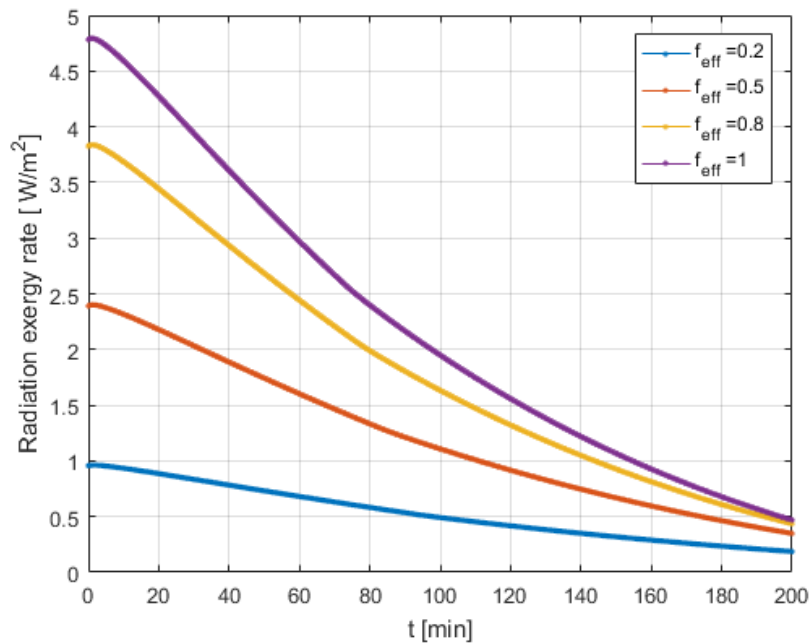


Figure 41. Radiation exergy transfer rate for different radiation area factors

f_{eff}	h_r [W/m²/K]
0.2	1.2
0.5	3
0.8	4.8
1	6

Table 3 Radiation heat transfer coefficient variation according to f_{eff}

In figure 42 is represented the exergy efficiency with an effective radiation area factor of 0.5. With respect to figure 30, where f_{eff} was assumed equal to 0.7, the area of

maximum efficiency has moved towards lower mean radiant and air temperatures. Indeed it can be noticed a general decrement of exergy efficiency at equal mean radiant and air temperature. The opposite situation happens with higher f_{eff} (figure 43).

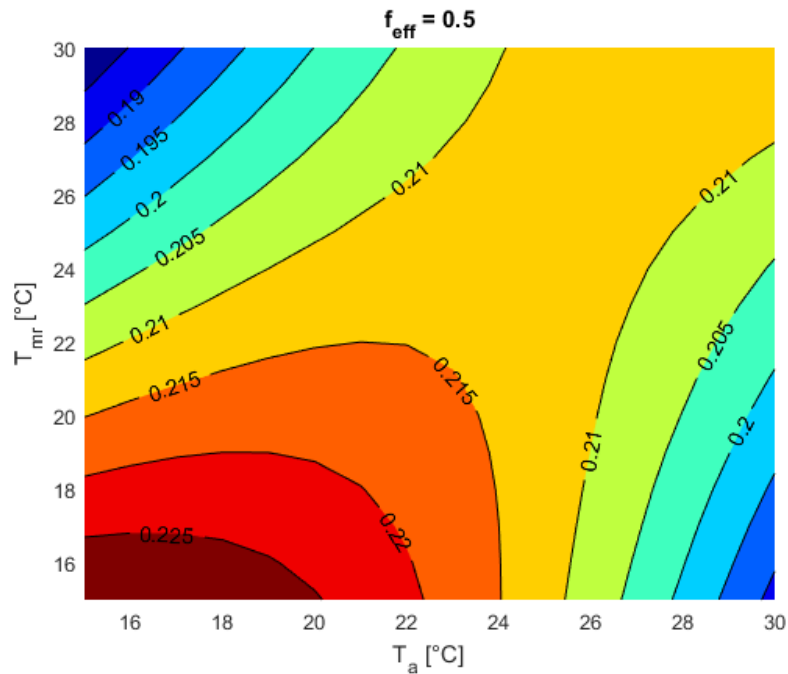


Figure 42. Exergy efficiency with $f_{eff} = 0.5$

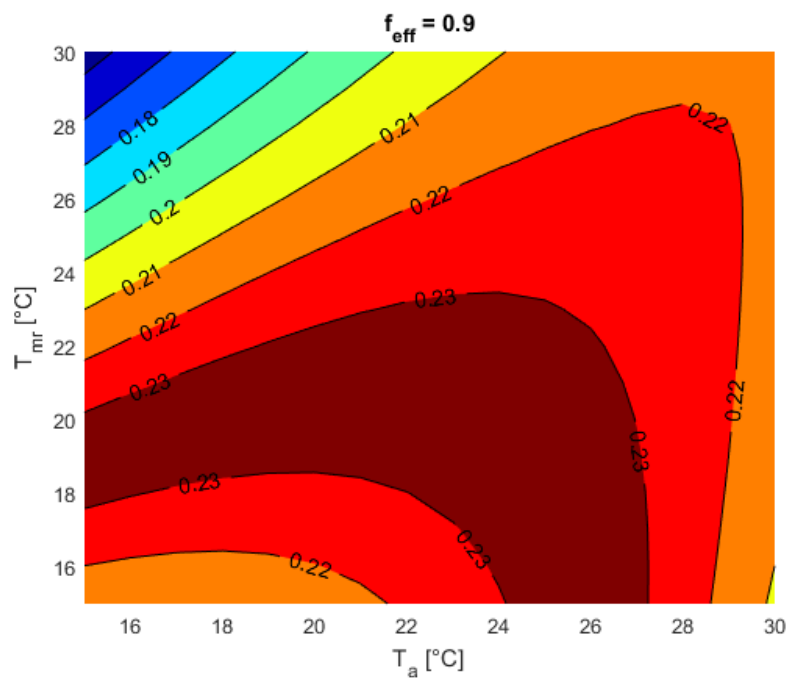


Figure 43. Exergy efficiency with $f_{eff} = 0.9$

In the first case, exergy efficiency distribution seems to be more uniform with respect to mean radiant and air temperature, even if the variation range remains larger with respect to air temperature and maximum exergy efficiency occurs always when air temperature is higher (or at most equal) than mean radiant temperature.

Looking at the PMV and exergy efficiency distributions, it is important to notice that with $f_{eff} = 0.5$, exergy efficiency does not coincide with neutral thermal comfort sensation, neither it happens when $f_{eff} = 0.9$ (figures 44 and 45).

Maximum exergy efficiency increase from around 22.5 % to 24 % with f_{eff} equal to 0.5 and 0.9 respectively; the PMV value correspondent to the maximum efficiency is around 0.05 in the first case, while it rises till 0.72 in the latter one. Hence, 0.4 variation of effective radiation area factor causes around 6 % increment in maximum exergy efficiency and 14 % increment of PMV.

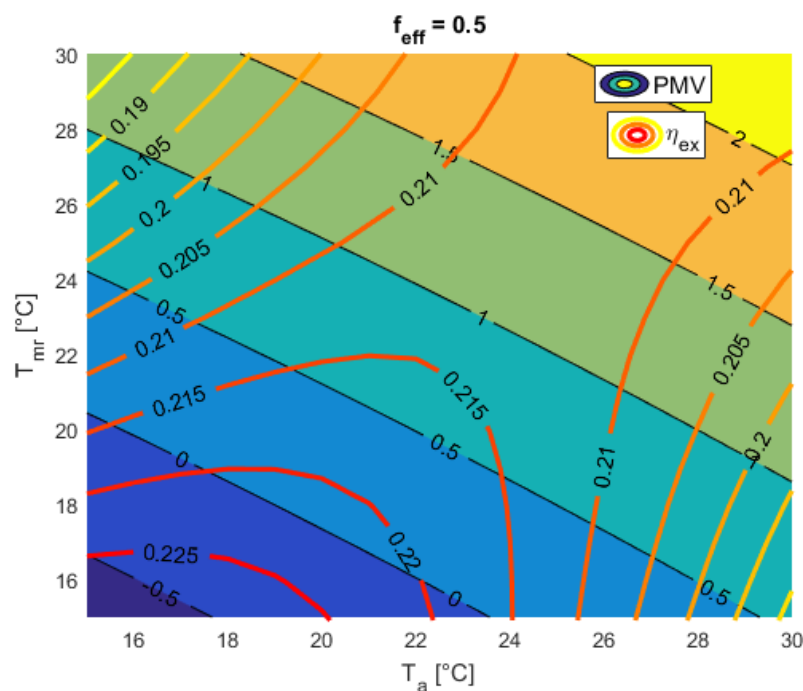


Figure 44. PMV and exergy efficiency with $f_{eff} = 0.5$

A middle value of f_{eff} between the two considered situations is 0.7 and in this case a coincidence between neutral PMV and maximum exergy efficiency occurs, as it has been analysed through section 5.2. This fact maybe could be seen as a further explanation of

the recorded usage of f_{eff} around 0.7 – 0.8 in the examined literature, and simulations seem to be in agreement with the choice.

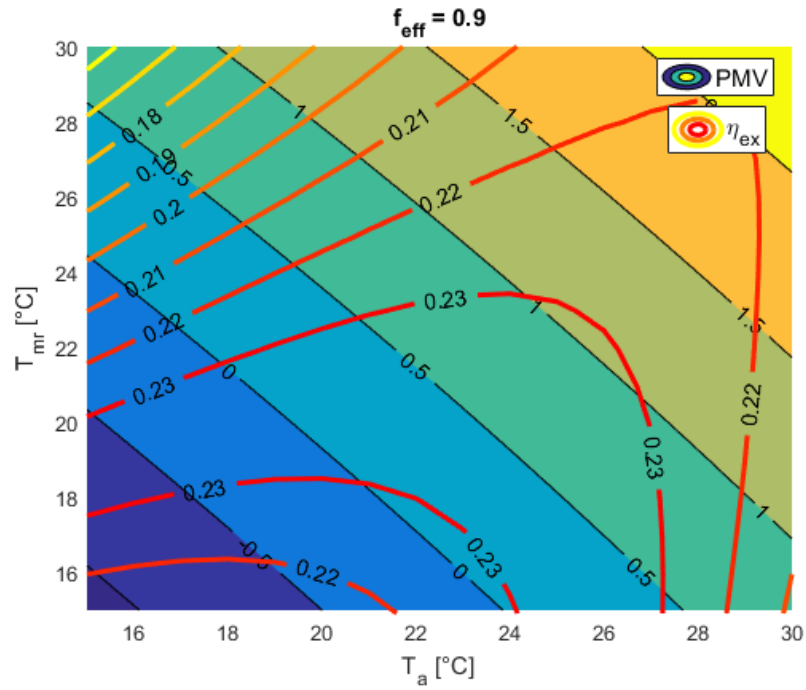


Figure 45. PMV and exergy efficiency with $f_{eff} = 0.9$

6. Conclusions

The presented research has given the analytical and numerical background to assess an unsteady state evaluation of body core and skin-layer temperature over time, with all their correlated quantities, when a human body system is exposed to an environment with well-known thermal characteristics. Starting from human body temperature previously described, a new definition of human body exergy efficiency has been given and the relationship with thermal comfort has been explored to find confirmations and discrepancies with respect to the previous exergetic analysis of human body in the built environment.

In the first part of the study, it has been confirmed that skin-layer temperature is strongly influenced by the surrounding thermal environment, while core temperature has a quasi-constant trend over time, whatever the exposure conditions are but with all the appropriate limits of the analysis.

Exergy efficiency increases over time, till a maximum stable value, dependent on the magnitude of energy and mass transfer processes between human body and environment. Considering different mean radiant and air temperatures, it has been recorded the occurrence of a maximum value of exergy efficiency, which indicates that may be a correlation between thermal comfort and exergetic analysis. Indeed, for given physiological condition, only one combination of environmental parameters ensures maximum exergy efficiency. It has been found that exergy efficiency never assumes values above 30 %, hence around 70 % of the exergy in input is destroyed in the energy and mass transfer processes and through basal metabolism.

Moreover, exergy efficiency distribution is not uniform with respect to mean radiant and air temperatures. Simulations demonstrate that at lower air temperature small changes in mean radiant temperature causes a large effect in exergy efficiency value, while moving towards higher air temperature this effect is much less pronounced. Therefore, because mean radiant temperature influences the radiation exergy transfer rate, we can conclude that human body is as sensible to radiation heat transfer rate as it is for the convective one.

The results obtained indicate that the maximum exergy efficiency coincides with a PMV between -0.5 and 0.5, hence with neutral thermal sensation.

Regarding thermal comfort, it is true that where the exergy efficiency is at the maximum value we find neutral thermal sensations, but the contrary statement cannot be affirmed. In fact, PMV could be within (-0.5, 0.5) range even with lower efficiencies. Probably mechanisms of physiological thermo-regulation have been not correctly taken into account or it hasn't been sufficiently considered the adaptation capacity of human body in its psychological dimension.

Finally, It is noteworthy that, when efficiency is not at its maximum but thermal comfort occurs, mean air temperature result to be always lower (or at most equal) than mean radiant temperature.

A sensitivity analysis on effective radiation area factor demonstrates a strong dependency of exergy efficiency and thermal comfort upon it. Pronounced variations occurs in exergy efficiency with relatively small changes in f_{eff} . Indeed, only in some cases maximum exergy efficiency area coincides with neutral thermal sensation and it occurs when effective radiation area factor is chosen around 0.7 – 0.8. Therefore, the recorded usage of these values for f_{eff} seems to be a realistic choice.

This analysis highlights the impact of environmental parameters on human body physiological processes and exergy efficiency. This approach could be useful to define the indoor parameters that ensure maximum efficiency and neutral thermal sensation. Through exergy analysis, it has been found out that convective and radiative heat transfer have almost the same influence on thermal comfort. It could be a good starting point for the development of heating/cooling regulation systems sensitive also to mean radiant temperature.

Exergetic analysis could be applied on HVAC systems and give important information about the identification of components' thermodynamic inefficiencies.

Therefore, applying exergy analysis on the whole system composed by HVAC and human body could become an essential instrument in the thermal design of the built environment, to provide the best indoor conditions for the occupants at the highest

exergy efficiency of human body and the lowest exergy consumption for HVAC systems, hence to move towards a more sustainable way to use energy.

References

- [1] J. Van Hoof, "Forty years of Fanger's model of thermal comfort: Comfort for all?," *Indoor Air*, vol. 18, no. 3, pp. 182–201, 2008.
- [2] M. Prek, M. Mazej, and V. Butala, "An approach to exergy analysis of human physiological response to indoor conditions and perceived thermal comfort," *7th Int. Therm. Manikin Model. Meet. Univ. Coimbra*, no. September, 2008.
- [3] J. M. Hensen, "On the thermal interaction of building structure and heating and ventilating system," Technische Universiteit Eindhoven, 1991.
- [4] ANSI/ASHRAE Standard 55, "Thermal Environment Conditions for Human Occupancy," 2004.
- [5] N. Djongyang, R. Tchinda, and D. Njomo, "Thermal comfort: A review paper," *Renew. Sustain. Energy Rev.*, vol. 14, no. 9, pp. 2626–2640, 2010.
- [6] P. O. Fanger, *Thermal comfort - Analysis and application in environmental engineering*. Copenhagen: Danish Technical Press, 1970.
- [7] A. P. Gagge, J. A. J. Stolwijk, and Y. Nishi, "An effective temperature scale based on a simple model of human physiological regulatory response," *Fac. Eng. Hokkaido Univ.*, 1972.
- [8] C. E. K. Mady, M. S. Ferreira, J. I. Yanagihara, and S. De Oliveira, "Human body exergy analysis and the assessment of thermal comfort conditions," *Int. J. Heat Mass Transf.*, vol. 77, pp. 577–584, 2014.
- [9] C. E. Keutenedjian Mady, M. Silva Ferreira, J. Itizo Yanagihara, P. Hilário Nascimento Saldiva, and S. de Oliveira Junior, "Modeling the exergy behavior of human body," *Energy*, vol. 45, no. 1, pp. 546–553, 2012.
- [10] M. Taleghani, M. Tenpierik, S. Kurvers, and A. Van Den Dobbelen, "A review into thermal comfort in buildings," *Renew. Sustain. Energy Rev.*, vol. 26, pp. 201–215, 2013.
- [11] B. M. Shukuya, M. Saito, K. Isawa, T. Iwamatsu, and H. Asada, "Low Exergy Systems for High-Performance Building and Communities 'Human body exergy balance and thermal comfort.'"
- [12] M. Prek and V. Butala, "Principles of exergy analysis of human heat and

- mass exchange with the indoor environment,” *Int. J. Heat Mass Transf.*, vol. 53, no. 25-26, pp. 5806–5814, 2010.
- [13] X. Wu, J. Zhao, B. W. Olesen, and L. Fang, “A novel human body exergy consumption formula to determine indoor thermal conditions for optimal human performance in office buildings,” *Energy Build.*, vol. 56, pp. 48–55, 2013.
- [14] M. M. Garcia, R. Y. Une, S. D. O. Junior, and E. K. Mady, “Exergy Analysis and Human Body Thermal Comfort Conditions : Evaluation of Different Body Compositions,” pp. 1–15, 2018.
- [15] A. Simone *et al.*, “A relation between calculated human body exergy consumption rate and subjectively assessed thermal sensation,” *Energy Build.*, vol. 43, no. 1, pp. 1–9, 2011.
- [16] M. Prek, “Thermodynamical analysis of human thermal comfort,” *Energy*, vol. 31, no. 5, pp. 732–743, 2006.
- [17] C. E. K. Mady, M. S. Ferreira, J. I. Yanagihara, and S. De Oliveira, “Human body exergy analysis and the assessment of thermal comfort conditions,” *Int. J. Heat Mass Transf.*, vol. 77, pp. 577–584, 2014.
- [18] X. Wang, “Thermal comfort and sensation under transient conditions,” 1994.
- [19] M. Shukuya, K. Tokunaga, M. Onoma, and Y. Itoh, “Calculation of Human-body Exergy Balance for Investigating Thermal Comfort under Transient Conditions,” *Proc. 7th Wind. Conf.*, no. April, 2012.
- [20] A. Quarteroni, F. Saleri, and P. Gervasio, *Scientific computing with MATLAB and Octave*, Fourth Edi. .
- [21] G. Riccardi, D. Pacione, and A. A. Rivellesse, *Manuale di nutrizione applicata*, 3rd ed. 2009.
- [22] M. Shukuya, “Calculation of Human Body-core and Skin-layer Temperatures under Unsteady-state Conditions,” no. November, 2015.
- [23] *ASHRAE Handbook of Fundamentals*. 2005.
- [24] H. Torío, A. Angelotti, and D. Schmidt, “Exergy analysis of renewable energy-based climatisation systems for buildings: A critical view,” *Energy Build.*, vol. 41, no. 3, pp. 248–271, 2009.
- [25] B. Kingma, “Human thermoregulation; A synergy between psysiology and

- mathematical modelling,” Maastricht University, 2012.
- [26] V. Verda and E. Guelpa, *Metodi Termodinamici per l'uso efficiente delle Risorse Energetiche*. Società Editrice Esculapio, 2015.
- [27] B. J. Arthur Harris and F. G. Benedict, “A Biometric Study of Human Basal Metabolism,” *Bull. Amer. Math. Soc*, vol. 23, pp. 233–236, 1914.
- [28] D. Fiala, K. J. Lomas, and M. Stohrer, “Modeling in Physiology,” *Society*, vol. 82, no. 5, pp. 1522–1536, 2008.
- [29] M. Prek and V. Butala, “Thermodynamic analysis of human physiological environmental conditions and perceived thermal comfort response to,” *Hum. Physiol.*, no. August, pp. 2008–2008, 2008.
- [30] C. E. K. Mady, M. S. Ferreira, J. I. Yanagihara, P. H. N. Saldiva, and S. Oliveira Junior, “Second law of thermodynamics and human body,” *Eng. Térmica (Thermal Eng.*, vol. 10, no. 01, pp. 88–95, 2011.
- [31] R. S. Damor, S. Kumar, and A. K. Shukla, “Numerical Solution of Fractional Bioheat Equation with Constant and Sinusoidal Heat Flux Condition on Skin Tissue,” *Am. J. Math. Anal.*, vol. 1, no. 2, pp. 20–24, 2013.
- [32] S. M. Becker, *Analytical Bioheat Transfer: Solution Development of the Pennes' Model*. Elsevier Inc., 2015.
- [33] M. Ferreira and J. Yanagihara, “A transient three-dimensional heat transfer model of the human body,” *Int. J. Heat Mass Transf.*, 2009.
- [34] C. E. K. Mady and S. Oliveira, “Human body exergy metabolism,” *Int. J. Thermodyn.*, vol. 16, no. 2, pp. 73–80, 2013.
- [35] M. Schweiker, M. Shukuya, and A. Wagner, “Analysis of human interactions together with human-body exergy consumption rate,” *7th Wind. Conf. Chang. Context Comf. an Unpredictable World*, no. April, pp. 12–15, 2012.
- [36] M. Shukuya, T. Iwamatsu, and H. Asada, “Development of human-body exergy balance model for a better understanding of thermal comfort in the built environment,” *Int. J. Exergy*, vol. 11, no. 4, p. 493, 2012.
- [37] A. Bejan, “CONSTRUCTAL LAW : DESIGN AS PHYSICS,” no. April, pp. 4–9, 2013.
- [38] L. Yang, Z. Nagy, P. Goffin, and A. Schlueter, “Reinforcement learning for optimal control of low exergy buildings,” *Appl. Energy*, vol. 156, pp. 577–586, 2015.

- [39] A. Angelotti and P. Caputo, "The exergy approach for the evaluation of heating and cooling technologies; first results comparing steady state and dynamic simulations," *Proc. 2nd PALENC 28th AIVC Conf.*, pp. 59–64, 2007.
- [40] T. Spircu and I. C. Carstea, "Numerical simulation of human thermal comfort in indoor environment 1 2," *Proc. 3rd WSEAS Int. Conf. FINITE Differ. - FINITE Elem. - FINITE Vol. - Bound. Elem.*, pp. 65–70, 2010.
- [41] B. Fan, X. Jin, X. Fang, and Z. Du, "The method of evaluating operation performance of HVAC system based on exergy analysis," *Energy Build.*, vol. 77, pp. 332–342, 2014.
- [42] M. Shukuya, "Exergetic review on thermal performance of window systems," *Proc. Glob. Conf. Energy Sustain. Dev.*, no. FEBRUARY, pp. 1–7, 2015.
- [43] M. Kepes Rodrigues, R. da Silva Brum, J. Vaz, L. A. Oliveira Rocha, E. Domingues dos Santos, and L. A. Isoldi, "Numerical investigation about the improvement of the thermal potential of an Earth-Air Heat Exchanger (EAHE) employing the Constructal Design method," *Renew. Energy*, vol. 80, pp. 538–551, 2015.
- [44] T. Hong, S. C. Taylor-Lange, S. D'Oca, D. Yan, and S. P. Corngnati, "Advances in research and applications of energy-related occupant behavior in buildings," *Energy Build.*, vol. 116, no. December, pp. 694–702, 2016.
- [45] F. Meggers, V. Ritter, P. Goffin, M. Baetschmann, and H. Leibundgut, "Low exergy building systems implementation," *Energy*, vol. 41, no. 1, pp. 48–55, 2012.
- [46] A. Hepbasli, "Low exergy (LowEx) heating and cooling systems for sustainable buildings and societies," *Renew. Sustain. Energy Rev.*, vol. 16, no. 1, pp. 73–104, 2012.
- [47] Z. Du, X. Jin, and B. Fan, "Evaluation of operation and control in HVAC (heating, ventilation and air conditioning) system using exergy analysis method," *Energy*, vol. 89, pp. 372–381, 2015.
- [48] U. Lucia, "The Gouy-Stodola theorem in bioenergetic analysis of living systems (irreversibility in bioenergetics of living systems)," *Energies*, vol. 7, no. 9, pp. 5717–5739, 2014.
- [49] Ş. Kilkış, "Exergy transition planning for net-zero districts," *Energy*, vol. 92, no. Part 3, pp. 515–531, 2015.

- [50] A. Yildiz and A. Güngör, "Energy and exergy analyses of space heating in buildings," *Appl. Energy*, vol. 86, no. 10, pp. 1939–1948, 2009.
- [51] M. Cianfrini, E. Sciubba, and C. Toro, "An exergy based method for the optimal integration of a building and its heating plant. part 1: Comparison of domestic heating systems based on renewable sources," *Proc. 25th Int. Conf. Effic. Cost, Optim. Simul. Energy Convers. Syst. Process. ECOS 2012*, vol. 7, no. September 2015, pp. 40–53, 2012.
- [52] A. Shaihidian, Z. Abbasi, V. Square, and H. Body, "Investigation of Effective Parameters on the Human Body Exergy and Energy Model," no. APRIL, pp. 8–9, 2015.
- [53] F. Meggers, M. Mast, and H. Leibundgut, "The missing link for low exergy buildings: low temperature-lift, ultra-high COP heat pumps," *Proc. Clima 2010 Sustain. Energy Use Build.*, no. JANUARY, 2010.
- [54] R. F. Rupp, N. G. Vásquez, and R. Lamberts, "A review of human thermal comfort in the built environment," *Energy Build.*, vol. 105, pp. 178–205, 2015.
- [55] M. Schweiker, S. Brasche, W. Bischof, M. Hawighorst, K. Voss, and A. Wagner, "Development and validation of a methodology to challenge the adaptive comfort model," *Build. Environ.*, vol. 49, no. 1, pp. 336–347, 2012.
- [56] U. Lucia, "Entropy generation: Minimum inside and maximum outside," *Phys. A Stat. Mech. its Appl.*, vol. 396, pp. 61–65, 2014.
- [57] M. Dovjak, M. Shukuya, and A. Krainer, "Connective thinking on building envelope - Human body exergy analysis," *Int. J. Heat Mass Transf.*, vol. 90, pp. 1015–1025, 2015.
- [58] T. Volk and O. Pauluis, "It is not the entropy you produce, rather, how you produce it," *Philos. Trans. R. Soc. B Biol. Sci.*, vol. 365, no. 1545, pp. 1317–1322, 2010.
- [59] K. Tokunaga and M. Shukuya, "Human-body exergy balance calculation under unsteady state conditions," *Build. Environ.*, vol. 46, no. 11, pp. 2220–2229, 2011.
- [60] U. Lucia, "Exergy flows as bases of constructal law," *Phys. A Stat. Mech. its Appl.*, vol. 392, no. 24, pp. 6284–6287, 2013.
- [61] U. Lucia and E. Sciubba, "From Lotka to the entropy generation approach," *Phys.*

A Stat. Mech. its Appl., vol. 392, no. 17, pp. 3634–3639, 2013.

- [62] M. Schweiker and M. Shukuya, “Adaptive comfort from the viewpoint of human body exergy consumption,” *Build. Environ.*, vol. 51, pp. 351–360, 2012.
- [63] K. Isawa and M. Shukuya, “Sensitivity Numerical Analysis of Human Body Exergy Balance under an Unsteady-State Thermal Environment—Behavioral Adaptation Induced by Undesirable Cold Storage by Building Envelope in Winter,” *Health (Irvine. Calif.)*, vol. 08, no. 08, pp. 737–748, 2016.
- [64] J. Coleman, E. Teitelbaum, H. Guo, J. Read, and F. Meggers, “Examining Architectural Air and Temperature with Novel Sensing Techniques,” *Energy Procedia*, vol. 122, pp. 1136–1141, 2017.
- [65] M. Dovjak, M. Shukuya, B. W. Olesen, and A. Krainer, “Analysis on exergy consumption patterns for space heating in Slovenian buildings,” *Energy Policy*, vol. 38, no. 6, pp. 2998–3007, 2010.
- [66] M. Shukuya, “Exergy concept and its application to the built environment,” *Build. Environ.*, vol. 44, no. 7, pp. 1545–1550, 2009.
- [67] J. A. Rabi, C. Elizabeth, and S. Fresia, “Thermal Comfort and Second-Law Analysis of Thermoregulation Mechanisms : Preliminary Considerations and Prospective Extensions,” *Proc. 11th Brazilian Congr. Therm. Sci. Eng. -- ENCIT 2006 Braz. Soc. Mech. Sci. Eng. -- ABCM, Curitiba, Brazil,- Dec. 5-8, 2006 Therm.*, pp. 1–10, 2006.

